

Transforming Design Spaces Using Pareto-Laplace Filters

Hazhir Aliahmadi,¹ Ruben Perez,² and Greg van Anders¹

¹*Department of Physics, Engineering Physics, and Astronomy,
Queen's University, Kingston ON, K7L 3N6, Canada*

²*Department of Mechanical and Aerospace Engineering,
Royal Military College of Canada, Kingston ON, K7K 7B4*

(Dated: March 4, 2024)

arXiv:2403.00631v1 [cs.CE] 1 Mar 2024

Abstract

Optimization is a critical tool for addressing a broad range of human and technical problems. However, the paradox of advanced optimization techniques is that they have maximum utility for problems in which the relationship between the structure of the problem and the ultimate solution is the most obscure. The existence of solution with limited insight contrasts with techniques that have been developed for a broad range of engineering problems where integral transform techniques yield solutions and insight in tandem. Here, we present a “Pareto-Laplace” integral transform framework that can be applied to problems typically studied via optimization. We show that the framework admits related geometric, statistical, and physical representations that provide new forms of insight into relationships between objectives and outcomes. We argue that some known approaches are special cases of this framework, and point to a broad range of problems for further application.

I. INTRODUCTION

Integral transforms serve an indispensable function in a broad range of engineering problems[1]. For example in signal processing [2] and control theory,[3] although the real world phenomena of interest play out in time, the structure of engineering systems and the design of systems is done in the frequency domain.[1] Similarly, in various engineering domains where behaviours are governed by waves, integral transforms can render more interpretable illustrations of the phenomena that facilitate engineering design[4]. The plurality of domains in which integral transforms are critical for engineering design raises the question of whether analogous approaches could provide similar levels of utility in other areas of engineering and design where they are not currently part of the standard practice.

The need for more sophisticated forms of analysis and understanding is particularly pressing in engineering domains that make extensive use of optimization. Optimization problems are notoriously difficult to solve [5] and solution algorithms frequently rely on techniques that obscure the underlying structure of the problem [6]. Although the situation is different in some case, for example gradient-based techniques (see, e.g., Ref. [7]) yield information about the local structure of the solution space, comprehensive, global pictures are more difficult to construct. The lack of clear relationships between the prob-

lem structure and the solution characteristics for many optimization problems raises a number of issues. Those issues include questions about sensitivity and future adaptability, among others.

Here, we describe an integral transform framework that can be applied to problems that are conventionally studied via optimization. The framework employs one or more objective functions to foliate the solution space to a design problem in terms of Pareto surfaces, and then applies a Laplace transform to the generalized volume of the surface. This “Pareto-Laplace” framework effectively filters the solution space by exponentially suppressing regions with large objective function values. As we show below, key features of the solution space yield identifiable effects in the Pareto-Laplace filtered form of the problem.

A key feature of the Pareto-Laplace framework is that it can be cast in equivalent geometric, statistical, and physical representations, which open avenues for powerful insight into the structure of underlying design problems. Geometrically, the Pareto-Laplace framework represents a filter on the solution space, where the Laplace variable scales the contributions from solutions based on their objective function values, analogous to a hyperbolic projection. Statistically, the Laplace transform serves as a moment-generating function (see, e.g., Ref. [8]), allowing for a probabilistic interpretation of the solution space volume, which can be computed without explicit knowledge of key quantities such as the minimum objective value or the volume function. Physically, it takes the form of a partition function in statistical mechanics (see, e.g., Ref. [9]), relating to thermodynamic concepts such as temperature and energy.

A second key feature of the framework is that its tripartite geometric/statistical/physical representation yields powerful computational approaches. The existence of means to explore solution spaces, e.g., via techniques including Monte Carlo and molecular dynamics simulation, means that it is possible to implement the filter on complex problems where the quantities that enter the formal definition of the filter are unknown.

A third key feature of the Pareto-Laplace filtration framework is that it is that related approaches to design and optimization problems emerge as special cases in certain limits. Special cases include simulated annealing [10], as well as statistical mechanics based materials design techniques such as digital alchemy [11] and gradient-based approaches.[12]

The remainder of this paper describes the structure of the Pareto-Laplace filter. We

motivate the filter based on general arguments, and then interpret the resulting mathematical quantities in geometric, statistical, and physical terms. We derive the effect of problem reparameterization on the structure of the filter. To build intuition about the structure of the framework we give explicit results for an example in linear programming where it is possible to compute the framework in closed form. Our primary interest is in applications of the filter in nonlinear and non-convex optimization problems, and example applications of the framework in problems ranging from naval architecture [13], land-use planning,[14, 15], as well prior applications in materials design,[11, 16] can be found in other works.

II. PARETO-LAPLACE FILTER

In this section, we motivate and derive the Pareto-Laplace filter from general arguments. We then give a trio of representations of the resulting mathematical expressions.

For illustrative purposes and to keep the development self-contained, we work first with a single objective function without constraints, before generalizing to an arbitrary number of objectives and/or constraints. Moreover, for the purposes of maintaining readability we avoid weighing down the description with rigorous proofs.

A. Motivation and Derivation

Consider an optimization problem

$$\min_{x \in \mathcal{S}} \mathcal{O}(x) \tag{1}$$

i.e., the minimization of some objective function \mathcal{O} over some set of possible design solutions $\{x\}$ in a solution space \mathcal{S} . A typical optimization algorithm aims to identify the solution of the problem x_* and determine $\mathcal{O}_{\min} \equiv \mathcal{O}(x_*)$, the objective at the minimum. However, this solution may not provide an answer to all design questions related to \mathcal{O} and \mathcal{S} .

Many issues, e.g., sensitivity analysis or algorithmic implementation, depend not only on the solution, but on the structure of the solution space. In general, for a given optimization problem, neither the optimal solution nor the structure of the solution space is

known. To determine the structure of the space, since we are interested in the space in the context of a specific optimization objective it strongly suggests we foliate the solution space by slices through the space for which \mathcal{O} is constant. We will refer to this as a Pareto slicing because surfaces or level sets in \mathcal{O} play a central role in Pareto-style approaches to optimization. Since the solution space must be geometrical in some sense, the basic notions of the structure of the space should be encoded by some geometric measure on the space. A very basic geometric measure is given by its volume. We are particularly interested in the volume of the Pareto slices that lie in a direction that is transverse to \mathcal{O} , so we will represent the volume of the solution space Ω as a function of the objective function

$$\Omega = \int d\mathcal{O} \Omega_{\perp}(\mathcal{O}) . \quad (2)$$

Armed with a primitive geometric measure of the solution space, it raises the problem of how to formulate a meaningful integral transform. In optimization, near-optimal solutions are likely to yield more useful information than highly sub-optimal ones. I.e., for many questions “good” solutions could be more instructive than “bad” ones, though the degree to which this is the case may vary (e.g., what counts as good or bad could be context dependent). Indeed, a systematic way of varying the tolerance for non-optimal solutions would provide an entry point for sensitivity analysis. Moreover, we should expect that in generic optimization problems, in the absence of constraints to the contrary, there will likely be far more “bad” potential solutions than “good” ones. Therefore one should expect Ω_{\perp} will grow with \mathcal{O} in generic cases. Anticipating Ω_{\perp} grows with \mathcal{O} , a functional filter should strongly suppress large- \mathcal{O} regions of \mathcal{S} .

Considering expectations of the relative value of “good” and “bad” solutions and together with the growth of Ω_{\perp} with \mathcal{O} suggests filtering the solution space via a Laplace transform of the form

$$Z(\beta) = \int_{\mathcal{O}_{\min}(\mathcal{C})}^{\infty} d\mathcal{O} e^{-\beta\mathcal{O}} \Omega_{\perp}(\mathcal{O}) , \quad (3)$$

where β plays the role of the Laplace variable, and \mathcal{O}_{\min} is the minimum possible value for the objective. Note Eq. (3) satisfies the criteria we outlined: the parameter $\beta > 0$ controls the relative contribution to Z from regions of \mathcal{S} with low- or high values of \mathcal{O} , and it exponentially suppresses solutions with large \mathcal{O} .

B. Geometric, Statistical, and Physical Representations

Eq. (3) gives a formal definition of the Pareto-Laplace filter. However, the key to the utility of the filter lies in the interpretation of $Z(\beta)$. In this subsection, we first consider the geometric aspects of the filter in more detail. We then find that this geometric representation suggests alternate statistical and physical representations. This trio of representations is a key to the Pareto-Laplace filter’s versatility and its use in illuminating how the solution space of a design problem is influenced by the design objectives (see Sec. III).

1. Geometric Representation

Since $\Omega(\mathcal{O})$ encodes the “volume” of potential design solutions that realize the design objective \mathcal{O} at some fixed level, the quantity $Z(\beta)$ aggregates those volumes to give a total volume of the solution space for all possible \mathcal{O} , however the contributions from solutions are scaled by a factor $\exp(-\beta\mathcal{O})$. In particular, a single solution at \mathcal{O} is suppressed relative to a solution at \mathcal{O}_{\min} by $w(\mathcal{O}) = e^{-\beta(\mathcal{O}-\mathcal{O}_{\min})}$. We sketch this schematically in Fig. 1 (see also Supplementary Movies S1 and S2).

We arrived at Eq. (3) by starting with an optimization defined over a solution space. Let us call the solution space \mathcal{S} . If we had N real, continuous design variables then we would have that $\mathcal{S} \subset \mathbb{R}^N$. If we take the objective function \mathcal{O} as a mapping $\mathcal{O} : \mathcal{S} \rightarrow \mathbb{R}$, then we define the solution landscape as a foliation of $(\mathcal{O}, \mathbf{x}_\perp) \in \mathcal{S}$ where \mathbf{x}_\perp lives on the $(N - 1)$ -dimensional space of foliations that are perpendicular to \mathcal{O} in \mathcal{S} .

Momentarily considering the specific case of linear programming provides valuable intuition. Considering a case where $\mathcal{O} = -\vec{C} \cdot \vec{x}$, in our geometric picture \mathcal{O} corresponds to the \vec{C} direction in \mathcal{S} , $\vec{C} \cdot \vec{x}_\perp = 0$, and $\Omega_\perp(\mathcal{O})$ corresponds to the volume of the feasible region along the Pareto fronts.

Returning to the general problem, as shown in Fig. 1 geometrically, Eq. (3) implements a filter on the solution space. It is possible to write a metric in the filtered geometry, which we will refer to as \mathcal{S}_β , as

$$ds^2 = d\mathcal{O}^2 + e^{-2\beta\mathcal{O}/(N-1)} ds_{\Omega_\perp}^2 \quad (4)$$

where ds is the line element in the filtered space, N is the number of dimensions in the solution space, and ds_{Ω_\perp} is the induced line element in the solution space that is orthog-

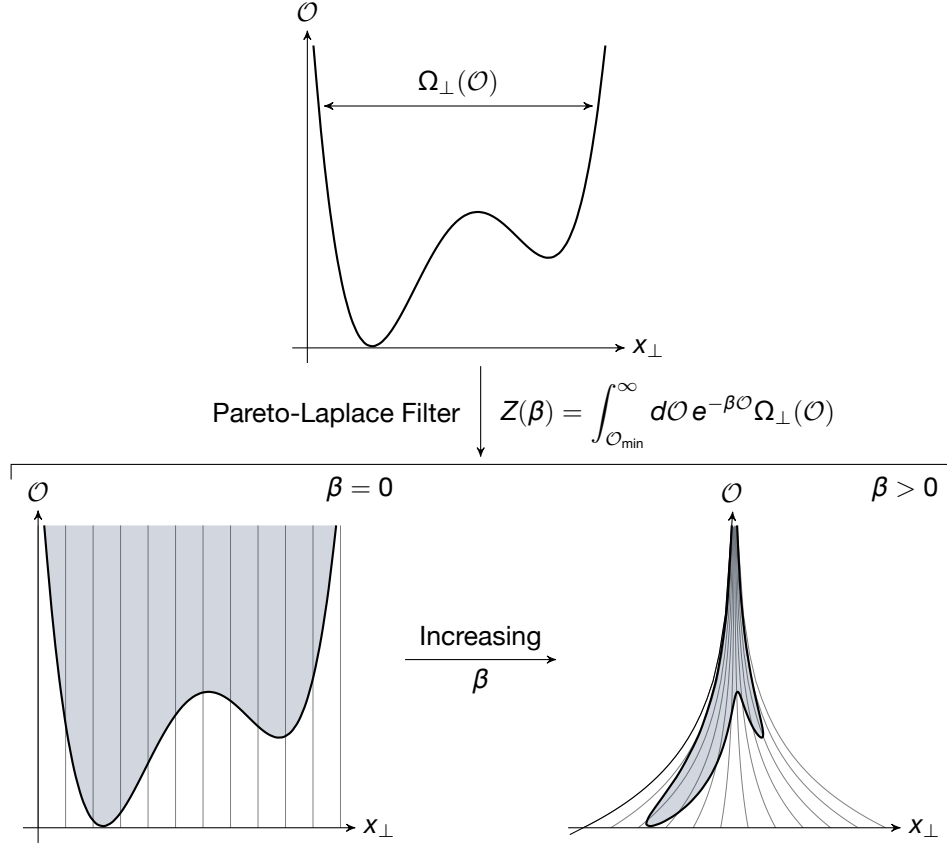


FIG. 1. Schematic representation of design landscape integral transform for a single design objective. (Top middle) A design problem exhibits a landscape of potential solutions distributed over a solution space \mathcal{S} in coordinates (\mathcal{O}, x_{\perp}) according to the level at which they satisfy the design objective \mathcal{O} and a set of other design variables x_{\perp} (represented here schematically as a single variable). There may be Ω_{\perp} solutions that satisfy the design objective at some fixed level \mathcal{O} . We propose to filter the solution space via the application of an integral transform, where Z computes the volume of the solution space depending on a parameter β that controls the degree of filtering of poor design solutions (which we take as large \mathcal{O}). For $\beta = 0$ (lower left) there is no filtering, however increasing β (lower right) effectively “pinches” the landscape for large \mathcal{O} . Increasingly large values of β leave effectively larger relative contributions from near optimal solutions, with only the optimal solution remaining in the limit $\beta \rightarrow \infty$.

onal to \mathcal{O} . The geometric nature of the filter is clarified by considering the coordinate transformation $\alpha = \frac{N-1}{\beta} \exp(\beta\mathcal{O}/(N-1))$, which gives the metric as

$$ds^2 = \frac{d\alpha^2 + ds_{\Omega_{\perp}}^2}{\alpha^2}, \quad (5)$$

which is a standard form for the metric of an N -dimensional hyperbolic space if the metric on the transverse space is flat, i.e. $ds_{\Omega_{\perp}}^2 = d\vec{x}_{\perp}^2$.

In light of Eq. (4), one can formally recover Eq. (3) by computing the volume measure on the filtered space,

$$d\omega = d\mathcal{O} d^{N-1}x_{\perp} e^{-\beta\mathcal{O}}, \quad (6)$$

and computing the volume $Z(\beta) = \int d\omega$ by integrating the solution space volume via foliation at a series of fixed \mathcal{O} .

Further technical geometric details relating the behavior of the objective function to the geometry of the solution space can be found in Appendices D and G, and on geodesics in \mathcal{S}_{β} can be found in Appendix C.

2. Statistical Representation

As we will show below, it is possible to explicitly compute $Z(\beta)$ for some problems, such as those in linear programming, explicit, closed-form evaluation is not feasible for many nonlinear and non-convex problems. In most optimization problems, we do not expect to have direct, a priori knowledge of \mathcal{O}_{\min} . Moreover, we do not expect to know $\Omega_{\perp}(\mathcal{O})$ explicitly. Given the lack of explicit knowledge of any of the key quantities that appear in Eq. (3) one might expect that, whatever its potential use, computing $Z(\beta)$ is inherently fraught.

However, we will note that the essence of the problem of computing Eq. (3) is to compute a volume. Computing volumes where direct integration is impractical is a standard problem in computational science, and there are many approaches to solving integration problems by recasting them in statistical language. E.g., it is a standard textbook exercise to use what is sometimes referred to as the ‘‘hit or miss’’ method (see, e.g. Ref. [17]) to estimate π by Monte Carlo integration.

Although basic algorithmic considerations could lead to a statistical representation of Eq. (3) it is more instructive to arrive at that perspective starting from an information

theoretic point of view. Information theory gives a recipe for constructing probability distributions with a given set of moments that make no other assumptions about the form of the distribution. That distribution is found by maximizing the entropy S with respect a probability distribution $p(x)$,

$$S = \int_{\mathcal{S}} d^N x p(x) \ln(p(x)) + \beta \left(\int_{\mathcal{S}} d^N x p(x) \mathcal{O}(x) - \langle \mathcal{O} \rangle \right) - \lambda \left(\int_{\mathcal{S}} d^N x p(x) - 1 \right), \quad (7)$$

where β is a Lagrange multiplier that enforces the moment constraint and λ is a Lagrange multiplier that enforces normalization. The maximization of Eq. (7) gives

$$p(x) = \frac{e^{-\beta \mathcal{O}}}{Z(\beta)}, \quad (8)$$

where

$$Z(\beta) = \int_{\mathcal{S}} d^N x e^{-\beta \mathcal{O}}. \quad (9)$$

Now, if we compute the integral by decomposing it as $d^N x = d\mathcal{O} d^{N-1} x_{\perp}$ and computing the integral over x_{\perp} , we obtain

$$Z(\beta) = \int_{\mathcal{O}_{\min}}^{\infty} d\mathcal{O} e^{-\beta \mathcal{O}} \Omega_{\perp}(\mathcal{O}). \quad (10)$$

Note that this is precisely the same form as Eq. (3) if we identify β , the Lagrange multiplier in Eq. (10), with β , the Laplace variable Eq. (3).

The connection between the geometric integral transform of optimization in Eq. (3) and the statistical interpretation of that quantity is not coincidental. In fact, for design problems in other areas of science and engineering, e.g., the design of self-assembled materials,[11, 16, 18–21] naval architecture,[22–24] and land-use planning, [14, 15] partition functions of the form Eq. (11) have been derived starting not from a geometric point of view, but from an information theoretic one.[8, 25]

3. *Physical Representation*

The deep connection between information theory and statistical mechanics [25] suggests the existence of a third, physical representation of the Pareto-Laplace filter in Eq. (3). $Z(\beta)$ can be identified as a partition function in statistical physics where $\beta = 1/T$, where T is thermodynamic temperature, \mathcal{O} plays the role of energy, \mathcal{O}_{\min} plays the role of

the ground state energy, and $\Omega(\mathcal{O})$ plays the role of the density of states, e.g. refer to Ref. [9].

The existence of a physical representation of the Pareto-Laplace filter has two important implications: one practical and one conceptual.

From the practical point of view, physics has developed a broad array of well-defined computational techniques, see, e.g. Ref. [26], that provide statistical sampling that can generate the distributions of $\{x\}$ that contribute to $Z(\beta)$ up to arbitrary accuracy even without a priori knowledge of the ground state energy and the density of states. The key to implementing these approaches is to recast Eq. (3) as

$$Z(\beta) = \int_{\mathcal{S}} d^N x e^{-\beta \mathcal{O}(x)} \quad (11)$$

where one does not assume that one has a priori knowledge of how to foliate \mathcal{S} in terms of \mathcal{O} . Given this framing, a very wide range of techniques can be used to sample the distributions that generate $Z(\beta)$ via techniques such as Monte Carlo (MC) and molecular dynamics (MD) simulation depending on the form of \mathcal{S} and $\mathcal{O}(x)$.

From the conceptual point of view, the fact that it is possible to impart Eq. (3) with a physical representation in terms of thermodynamics points to one of the advantages of thermodynamics as a description of systems of many degrees of freedom: it abstracts the complex interplay of the many degrees of freedom in terms of concrete, tangible mechanical effects such as pressure, stress, strain, etc. Aspects of this perspective have been developed starting from the statistical representation of this framework in materials design under what the authors of Ref. [11] termed “digital alchemy” and in the context of networks under what the authors of [22] termed “systems physics”.

C. Symmetry and Problem Reformulation

The solution space filter Eq. (3) provides considerable information about the structure of the underlying design problem. However, for many problems, it is possible to formulate them in multiple ways (e.g., via different choices of parameters or units), and it is therefore crucial to understand how such problem reformulations affect the information that the transform yields.

1. Translation

One way of reformulating the design problem would be to shift coordinates in \mathcal{S} via a constant. Two cases are instructive.

If the coordinate transformation has the form

$$\mathbf{x}_\perp \rightarrow \mathbf{x}_\perp + \Delta\mathbf{x}_\perp \quad \mathcal{O} \rightarrow \mathcal{O}, \quad (12)$$

i.e., there is a shift in the transverse directions that leaves the objective unchanged, then in Eq. (3) the measure and the scaling factor are invariant, and $\Omega_\perp \rightarrow \Omega_\perp$ so it is also invariant. As a result, $Z(\beta) \rightarrow Z(\beta)$, which means that Eq. (3) preserves all information under transverse translation.

If the coordinate transformation has the form

$$\mathbf{x}_\perp \rightarrow \mathbf{x}_\perp \quad \mathcal{O} \rightarrow \mathcal{O} + \Delta\mathcal{O}, \quad (13)$$

i.e., there is a shift in the objective that leaves the transverse directions unchanged, then in Eq. (3) the measure and $\Omega_\perp \rightarrow \Omega_\perp$ are invariant, however with the scaling factor $e^{-\beta\Delta\mathcal{O}}$. As a result, $Z(\beta) \rightarrow e^{-\beta\Delta\mathcal{O}}Z(\beta)$. The effect of this scaling factor is to shift appropriate moments of \mathcal{O} by $\Delta\mathcal{O}$, however, it preserves the rest of the structure of $Z(\beta)$.

2. Rotation

In addition to translation, consider rotation in \mathcal{S} . Rotations that correspond to coordinate transformations on \mathcal{S} that do not alter the objective function preserve Ω_\perp , the measure, and scaling factor in the transform. Hence $Z(\beta) \rightarrow Z(\beta)$, so the transform preserves information under rotations that do not alter the objective.

3. Rescaling

Finally, it is instructive to consider rescaling the objective. Objective rescaling could arise if, say, an objective was reformulated in different units.

Consider $\mathcal{O} \rightarrow \alpha\mathcal{O}$. This transformation preserves Ω_\perp , however, the measure and scaling factor are not invariant. However, we note that applying this rescaling in Eq. (3) gives $Z(\beta) \rightarrow \frac{1}{\alpha}Z(\beta/\alpha)$. That means that up to a constant overall rescaling of $Z(\beta)$ and a rescaling $\beta \rightarrow \beta/\alpha$ the transform preserves all information about the design space.

D. Generalizations

For simplicity we developed the theory above for problems with a single objective and no constraints and a continuous \mathcal{S} . In this section we relax these assumptions.

1. Multi-Objective Problems

We are interested in problems where we can have multiple objectives. Given the multiple representations of the design filter that we identified in the case of a single objective function, there are several equivalent routes one could take that to develop an analogous theory for multiple design objectives. We will give one line of argument that requires a minimal amount of mathematical formalism and leave the description of derivations via other approaches to other work.

For those multi-objective problems it is useful to foliate the solution space \mathcal{S} according to set of M design objectives \mathcal{O}_i , where we are interested in the volume of the solution space where each of the \mathcal{O}_i is fixed $\Omega_{\perp}(\{\mathcal{O}_i\})$. In principle it would be useful to implement a filter of Ω according to each of the design objectives. We therefore write

$$Z(\{\beta_i\}) = \left[\prod_{i=1}^M \int_{\mathcal{O}_{\min}^{(i)}}^{\infty} d\mathcal{O}_i e^{-\beta_i \mathcal{O}_i} \right] \Omega_{\perp}(\{\mathcal{O}_i\}) . \quad (14)$$

We can interpret $Z(\{\beta_i\})$ as a volume on the space with the line element

$$ds^2 = \sum_{i=1}^M d\mathcal{O}_i^2 e^{-\frac{2}{N-1} \sum_{j \neq i} \beta_j \mathcal{O}_j} + e^{-\frac{2M}{N-1} \sum_{i=1}^M \beta_i \mathcal{O}_i} dx_{\perp}^2 , \quad (15)$$

which gives the volume element

$$d\omega = \left[\prod_{i=1}^M d\mathcal{O}_i e^{-\beta_i \mathcal{O}_i} \right] d^{N-M} x_{\perp} . \quad (16)$$

One can recover Eq. (14) by integrating $d\omega$ over \mathcal{S} by integrating each slice of x_{\perp} .

Note that, like the single objective case, it is a straightforward exercise in information theory to derive Eq. (14) via entropy maximization.

It is useful to remark briefly on the interpretation of various quantities that are computable from Eq. (14). It will not be surprising since the single objective Eq. (3) admitted

geometrical, statistical, and physical interpretations, the multi-objective case yields a similar range of interpretations. Some multi-objective applications of this framework have been described in other work, e.g. Refs. [14, 15, 20, 22].

It is important to note that although we are considering examples in which there are multiple objectives at play, the focus of our analysis was on the form of the solution space as “scored” by the various objectives of interest. However, it is important to note that in the treatment of the multi-objective case, at no point in the analysis were we forced to write a single overall objective function. In this sense, our analysis is more general than optimization and is not predicated on the choice of any one particular form for the optimization problem. It is therefore possible to situate many different formulations optimization problems involving the same set of objectives in the context of this framework. Indeed, that could be regarded as one of the strengths of the present approach.

2. Constraints

Until this point, we’ve avoided a detailed discussion of constraints, however they are straightforward to incorporate into this framework. For inequality constraints, one must simply cast constraints in the form

$$g_\gamma(x) > 0 \tag{17}$$

and multiply the integrand in Eq. (3) or Eq. (14)

$$G(x) = \prod_{\gamma} \theta(g_\gamma(x)) , \tag{18}$$

where $\theta(\cdot)$ is the unit step function. The case of equality constraints can be handled by formulating them so that

$$h_\delta(x) = 0 \tag{19}$$

and multiplying the transform integrand by

$$D(x) = \prod_{\delta} \delta(h_\delta(x)) \tag{20}$$

where $\delta(\cdot)$ is the Dirac delta function.

Readers may recognize that constraints could simply be absorbed into the definition of \mathcal{S} , however in cases where solving the constraints is difficult, it could be more profitable to define \mathcal{S} as unconstrained and write an explicit set of constraints. In this case,

notationally it would make sense to write the volume of the solution space foliation as

$$\Omega_{\perp}(\{\mathcal{O}_i\}) \rightarrow \Omega_{\perp}(\{\mathcal{O}_i\}, \{\kappa_{\alpha}\}) , \quad (21)$$

where $\{\kappa_{\alpha}\}$ are some parameters describing the constraints.

Readers may also recognize there is nothing to stop one from using the transform framework to study the structure of the solution space as a function of the constraints alongside or instead of as a function of objectives. Constraint-based transformations also yield relationships among moments that provide leverage. Indeed, there are cases in which performing a transformation with respect to a constraint provides very useful information about the structure of the solution space; see, e.g., Refs. [18, 27].

Note, viewing the Pareto-Laplace framework from the physics perspective, it is also straightforward to incorporate constraints using Lagrange multiplier methods. Using Lagrange multipliers to invoke constraints can be implemented simply by performing a Legendre transform (see, e.g., Ref. [28] for a detailed description of Legendre transforms in conventional, statistical physics settings). This approach has been applied in prior works that use the Pareto-Laplace framework in specific cases, e.g. Refs. [11, 18, 27].

3. Discrete Cases

Many problems of interest involve discrete spaces; e.g., instead of $\mathcal{S} \in \mathbb{R}^N$ those problems have $\mathcal{S} \in \mathbb{Z}^N$. The theory we described above carries over straightforwardly to that case. In particular, Eq. (3) retains its form, the only difference is that $\Omega_{\perp}(\mathcal{O})$ rather than being a continuous volume is a sum of delta-functions at each allowed discrete value of \mathcal{O} where the coefficient of the delta function is the discrete number of solutions in \mathcal{S} with that value of \mathcal{O} .

Notions we developed in the continuum about, e.g., moments, including their geometric, statistical, and physical interpretation all carry over to the discrete case. The only difference is that in the discrete case, these notions refer to sets of points in space rather than a continuum volume.

Continuum intuition about modes in $Z(\beta)$ that arise collectively from dense regions in \mathcal{S}_{β} also have meaning in discrete cases if one interprets density in \mathcal{S}_{β} as a smeared-out version of density over a region of \mathcal{S}_{β} . One can see this by realizing that in the discrete

case, in essence each point in \mathcal{S} is the source of a microscopic mode in $Z(\beta)$, and that notions of adjacency in \mathcal{S} can be interpreted collectively in terms of modes in \mathcal{S}_β that contribute to $Z(\beta)$.

III. DESIGN ANALYSIS

To better understand how the Pareto-Laplace filter encodes information about the design problem we use $Z(\beta)$ to compute design information about moments of \mathcal{S}_β , aspects of the transverse geometry, and consider questions of solution robustness.

A. Moments: Geometrical, Statistical, and Physical Aspects

Given the geometric interpretation of Eq. (3) as the volume of a solution space projection, the quantity

$$\langle \mathcal{O} \rangle = \frac{1}{Z(\beta)} \int_{\mathcal{O}_{\min}}^{\infty} d\mathcal{O} e^{-\beta \mathcal{O}} \Omega_{\perp}(\mathcal{O}) \mathcal{O} = -\frac{\partial \ln Z(\beta)}{\partial \beta}, \quad (22)$$

can be interpreted as the geometric centroid of the transformed solution space, called \mathcal{S}_β . Eq. (22) is precisely the statistical expectation for \mathcal{O} via Eq. (7). This indicates that $Z(\beta)$ plays the role of a moment-generating function for \mathcal{S}_β .

Note that in geometric, statistical, and physical settings, moments provide key information about the representative entities they describe. Geometrically, Eq. (22) describes a centroid, whereas statistically it represents an expectation value for samples drawn uniformly on \mathcal{S}_β . Physically, Eq. (22) represents a thermal expectation value.

This intuition generalizes to cases with multiple objective functions. For multi-objective cases

$$\langle \mathcal{O}_i \rangle = -\frac{\partial \ln Z}{\partial \beta_i} \quad (23)$$

remains a geometric centroid, an expectation value, and a thermal average for \mathcal{O}_i . Likewise, higher-order moments

$$\sqrt{\langle \mathcal{O}_i^2 \rangle - \langle \mathcal{O}_i \rangle^2} = \sqrt{\frac{\partial^2 \ln Z}{\partial \beta_i^2}} \quad (24)$$

represent characteristic sizes, as well as being related to statistical variances, and thermal susceptibilities. Additionally, because the multiple objectives supply added dimensions,

it is possible to compute additional moments

$$\langle \mathcal{O}_i \mathcal{O}_j \rangle - \langle \mathcal{O}_i \rangle \langle \mathcal{O}_j \rangle = \frac{\partial^2 \ln Z}{\partial \beta_i \partial \beta_j} \quad (25)$$

that also encode aspects of the geometry of the solution space.

In mechanics, moments of the form Eq. (25) relate to angular motion, hence if the geometry of the solution space has the form of a spherical top this implies a strong symmetry of the geometry of the projected S for given values of β_i . Statistically, that would imply a lack of statistical correlation among the deviations of solutions from average objective values. Moments that deviate from sphericity indicate hierarchical relationships among objectives (i.e. that some have more variability than others), or that one or more objectives are acting in concert or opposition to one another. Statistically, these would manifest in terms of variance/covariance or correlation functions that follow taking the point of view that Eq. (25) defines a covariance matrix.

However, the physical representation of Eq. (14) also indicates that moments of the form Eq. (25) can be thought of as treating the transformed solution space as a piece of physical material and determining the physical deformation of it to the application of anisotropic pressure. Depending on the form of Eq. (25) the solution space could behave like an isotropic fluid (highest symmetry) or an anisotropic, shear-supporting solid (least symmetry).

Each of these perspectives provides a window on questions of sensitivity, either in terms of the “squishiness” of the solution space, it’s geometric dispersion, or its statistical covariance, that could provide useful insight depending on the fluency of the practitioner and the problem in question. The diversity of perspectives and the problems to which they could be applied is too large to provide a representative survey here. Some of these perspectives have been treated in special cases of this approach applied to materials design and naval architecture, e.g. Refs. [11, 23].

B. Transverse Geometry

The foregoing description of the solution space focused on geometric, statistical, and physical understanding of the space as projected on an axis that corresponds with the design objective \mathcal{O} . However, although the quality of a design solution is captured in

terms of \mathcal{O} , the form of form of the solution is mostly specified in the transverse directions in \mathcal{S} . Hence, knowledge of the geometric form of \mathcal{S} in the transverse space is crucial to questions about the structure of a design and its realization.

1. Coarse Graining

Understanding the geometry of the transverse space is most useful and challenging in the case where the dimensionality of \mathcal{S} is large. In those situations it is useful [23] to identify some overall characteristics of putative design solutions (which could be a composite of basic design elements) and to examine projections of the solution space geometry onto those coordinates.

To enact this, one can start with $Z(\beta)$ in the form Eq. (9) introduce a foliation of \mathcal{S} in terms of both \mathcal{O} and some design characteristic \mathcal{C} . This yields

$$Z(\beta) = \int d\mathcal{C} \int d\mathcal{O} e^{-\beta\mathcal{O}} \Omega_{\perp}(\mathcal{O}, \mathcal{C}), \quad (26)$$

where $\Omega_{\perp}(\mathcal{O}, \mathcal{C})$ is the volume of the slice in \mathcal{S} that is transverse to both \mathcal{O} and \mathcal{C} .

In physics terminology, Eq. (26) implements a version of coarse-graining because it effectively “lumps together” a set of states by providing a description that does not explicitly depend on some of the properties of the states. In conventional physical settings, this approach is extremely powerful (see, e.g., Ref. [29]).

To enact this approach, it is convenient to work in terms of the so-called Landau free energy, $F(\beta, \mathcal{C})$. The Landau free energy is given by

$$e^{-\beta F(\beta, \mathcal{C})} = \int d\mathcal{O} e^{-\beta\mathcal{O}} \Omega_{\perp}(\mathcal{O}, \mathcal{C}), \quad (27)$$

so that

$$Z(\beta) = \int d\mathcal{C} e^{-\beta F(\beta, \mathcal{C})}. \quad (28)$$

In this form, the Landau free energy encodes an effective volume of the solution space projected onto the direction of \mathcal{C} . Note that although we are filtering the space in the \mathcal{O} direction, Eq. (27) computes the effect of the \mathcal{O} filter on a different characteristic of the design, \mathcal{C} .

It can be particularly useful to examine the transverse geometry in cases with multiple design objectives. For ease of illustration, we will consider two objectives, but the generalization to an arbitrary number of objectives is straightforward.

For two objectives we can redevelop Eq. (26) to get

$$Z(\beta_1, \beta_2) = \int d\mathcal{C} \int d\mathcal{O}_1 \int d\mathcal{O}_2 e^{-\beta_1 \mathcal{O}_1 - \beta_2 \mathcal{O}_2} \Omega_{\perp}(\mathcal{O}_1, \mathcal{O}_2, \mathcal{C}) . \quad (29)$$

We can similarly consider the quantity

$$e^{-\beta F(\beta_1, \beta_2, \mathcal{C})} = \int d\mathcal{O}_1 \int d\mathcal{O}_2 e^{-\beta_1 \mathcal{O}_1 - \beta_2 \mathcal{O}_2} \Omega_{\perp}(\mathcal{O}_1, \mathcal{O}_2, \mathcal{C}) . \quad (30)$$

Eq. (30) plays an important role in algorithmic implementations of this framework and for interpretation. In stochastic approaches to optimization, particularly those that involve Markov Chains, $-\nabla F(\beta_1, \beta_2, \mathcal{C})$ is an effective force in the solution space for the sampling algorithm. In deterministic approaches, $-\nabla F(\beta_1, \beta_2, \mathcal{C})$ encodes an average gradient across \mathcal{S}_{β} at fixed \mathcal{C} . Eq. (30) thus encodes basic aspects of flows in algorithms. But because those flows are affected by the competing pressures $\beta_{1,2}$, Eq. (30) is also important for quantifying and interpreting trade-offs among objectives.

2. Consequences of Objective Trade-Offs

Since Z retains its geometrical, statistical, and physical character in the representation Eq. (26), so Eq. (30) reduces the effect of the competing pressures for objectives in terms the characteristic \mathcal{C} . This means that Eq. (30) encodes the structure of the design spaces as viewed from the perspective of the design characteristic \mathcal{C} . Consequently, an analogous set of arguments can be employed to quantify the geometry in terms of \mathcal{C} as we showed for \mathcal{O} . In particular $\langle \mathcal{C} \rangle$ and $\langle \mathcal{C}^2 \rangle - \langle \mathcal{C} \rangle^2$ are geometrical and statistical moments. Importantly, these moments are functions of $\beta_{1,2}$, which means they express a relationship between some characteristic design feature and the relationship among the design objectives. These sorts of trade-offs have been evaluated in detail in, e.g., Ref. [15].

3. Effective Landscapes and Design Phases

An additional useful insight from expressions of the form of Eq. (30) (and generalizations) is that they quantify the effective form of the solution landscape as a function of one or more design characteristics of interest. Because Eq. (30) is explicitly a function of the competing design pressures, it encodes significant information about the structure of

the solution space both near global minima and away from them. In physics applications quantities of this form are used to construct phase diagrams that can distinguish distinct forms of the overall behaviour of systems with macroscopically large numbers of degrees of freedom. The existence of expressions of the form of Eq. (30) in design settings indicates that similar approaches can be applied to identify analogues of phases in design problems. Particular cases of this have already emerged in problems in land-use planning [14] and in naval architecture.[22]

In presenting the framework although we could be agnostic about the precise form of the design objectives and design characteristics, for the purposes of interpretation we drew a conceptual distinction between them. However, from a purely mathematical point of view, there is no reason why one could not develop the framework above with the roles of the design objectives and an appropriately quantified set of design characteristics reversed. In this way, the various geometric, statistical, and physical lenses that can be used to focus on relationships between objectives and characteristics could be used in both directions. In colloquial terms, the approach we presented boils down to “slicing” and “pinching” the solution space in a systematic way. The only thing that separates the application of this framework to optimization or inverse optimization problems is “angle” of the slicing.

C. Robustness

1. Near-Optimal Designs

In many practical optimization problems, there is a limitation, e.g. finite precision, that drives a mismatch between an as-designed optimal solution and an as-realized real-world implementation. If any realization will inevitably miss the ideal target, targets that are relatively more robust are ones for which there exists a greater number of ways to have a near miss than ones in which there are few ways to have a near miss. Hence basic questions about the robustness of a putative solution depend on the near-optimal form of S_β .

To understand how this form of robustness is captured by the Pareto-Laplace filter, consider a hypothetical situation in which there is a unique solution of the optimization

problem. If there is a unique solution at some \mathcal{O}_{\min} , then the volume of the solution space Ω_{\perp} will vanish for $\mathcal{O} < \mathcal{O}_{\min}$. In that case, suppose that for values of the compliance that fall just above \mathcal{O}_{\min} we can approximate the phase space volume

$$\Omega_{\perp}(\mathcal{O}) = \gamma(\mathcal{O} - \mathcal{O}_{\min})^{N_{\text{IP}}/\nu-1}, \quad (31)$$

where γ , N_{IP} , and ν are constants. What are they?

If the design problem has many variables (i.e. the dimensionality of $\mathcal{S} \gg 1$), it is not a priori clear that all of those variables will be equally free near an optimal design. It could be that some number of those variables are “locked in” and some of them are “in play”. This asymmetry between design variables could originate from many sources: the unequal distribution of the effects of constraints among the design variables or the existence of inhomogeneity in the specification of the design objectives, among others. Regardless of the source, the effective dimensionality of \mathcal{S} near \mathcal{O}_{\min} could be less than the full dimensionality of \mathcal{S} for $\mathcal{O} \gg \mathcal{O}_{\min}$. This can also be thought of in physical terms: some of the degrees of freedom may “condense” for the design to enter the region of \mathcal{S} in which \mathcal{O} is below some threshold, and the behaviour near \mathcal{O}_{\min} might entail condensation of only the remaining degrees of freedom.

By this dimensional argument, the parametric growth of the near-optimal Ω_{\perp} will be controlled by the number of degrees of freedom that are “in-play” near the minimum. Hence, N_{IP} counts the effective number of degrees of freedom that exhibit variation near optimality. The parameter ν reflects how the objective function depends on variation in the degrees of freedom. For example, for linear dependence $\nu = 1$ whereas for quadratic dependence $\nu = 2$ (see Appendix I). The coefficient γ is a geometric prefix that encodes the scaling of the growth.

Given this identification, it is possible to Eq. (3) directly in the limit of large β (small T)

$$Z(\beta) \propto \frac{e^{-\beta\mathcal{O}_{\min}}}{\beta^{N_{\text{IP}}/\nu}}, \quad (32)$$

where we have dropped negligible overall multiplicative constants. That means that in the limit of large β or, equivalently, low temperature T , we can estimate Eq. (22) to be

$$\langle \mathcal{O} \rangle \approx \mathcal{O}_{\min} + \frac{N_{\text{IP}}}{\nu} T. \quad (33)$$

Eq. (33) is an important relation. In particular, it may not be a priori clear which degrees of freedom are in play near optimality. Indeed, especially in non-linear problems,

there may exist a complex set of correlations among degrees of freedom that obscure the forms of variability that can exist. Eq. (33) indicates that if there exists a means to evaluate $\langle \mathcal{O} \rangle$ near $T = 0$ the slope of the curve determines the number of degrees of freedom that are in play.

This can be viewed as a measure of robustness because it quantifies the space available for “near misses”. To see this, as the limit $\beta \rightarrow \infty$ or $T \rightarrow 0$ is approached, non-optimal solutions are effectively filtered out, while near this limit, i.e., for sufficiently large β or sufficiently small T the geometry of the solution space leaves a clear imprint on the moments. Note that similar reasoning can extend this beyond the small T (large β) limit. The analysis of such cases, which we give in Appendices B and G, shows that changes in the rate of growth of $\Omega_{\perp}(\mathcal{O})$ yield identifiable effects on the behavior of $\langle \mathcal{O} \rangle$. Because these moments can be computed in algorithmic implementations of the Pareto-Laplace filter, it is possible to obtain key information about \mathcal{O}_{\perp} even if it is not known directly.

2. Modes

One of the key conceptual outcomes of integral transforms in signal, control, and other problems is the identification of characteristic modes of the system. Here we derive analogous modes in the Pareto-Laplace framework.

Consider a situation in which there is a large density of solutions in \mathcal{S} at some value of the design objective \mathcal{O}_* that fall in the vicinity of some x_{\perp}^* in the transverse space. It is instructive to consider the contribution that these states would make to $Z(\beta)$, which we will write as $Z_*(\beta, \mathcal{O}_*)$, which has the form

$$Z_*(\beta, \mathcal{O}_*) = \int_{\mathcal{O}_{\min}(\mathcal{C})}^{\infty} d\mathcal{O} e^{-\beta\mathcal{O}} \delta(\mathcal{O} - \mathcal{O}_*) \int_{V_*} d^{N-1}x_{\perp} \rho(x_{\perp}), \quad (34)$$

where $\delta(\cdot)$ is the Dirac delta-function, V_* is the volume of the transverse space near x_{\perp}^* , and $\rho(x_{\perp})$ is the density of states on the region. If $\rho(x_{\perp})$ is sufficiently well behaved over the region that one can employ the mean value theorem, then Eq. (34) reduces to

$$Z_*(\beta, \mathcal{O}_*) = e^{-\beta\mathcal{O}_*} \bar{\rho} V_*, \quad (35)$$

where $\bar{\rho}$ is the mean density of $\rho(x_{\perp})$ over the region.

Eq. (35) indicates that $Z(\beta)$ encodes critical information about the solution space, in general. To see this, note for fixed \mathcal{O} , the regions in the solution space that contribute

most to $Z(\beta)$ are the ones that are most dense. Also note that for fixed density, the regions of the space that fall off most slowly in β are the ones for which \mathcal{O} is the smallest.

Another way of viewing this is by passing to the physical representation by working in terms of T in which case Eq. (35) becomes

$$Z_*(T, \mathcal{O}_*) = e^{-\mathcal{O}_*/T} \bar{\rho} V_* . \quad (36)$$

We can compare the relative contribution of two regions of identical density and volume at two different values of the objective $\mathcal{O}_*^{(1)}$ and $\mathcal{O}_*^{(2)}$ at fixed temperature as

$$\frac{Z_*(T, \mathcal{O}_*^{(1)})}{Z_*(T, \mathcal{O}_*^{(2)})} = e^{(\mathcal{O}_*^{(2)} - \mathcal{O}_*^{(1)})/T} , \quad (37)$$

Note that Eq. (37) is greater than one if $\mathcal{O}_*^{(1)} < \mathcal{O}_*^{(2)}$. In other words, at any temperature, if two regions of \mathcal{S} have the same volume and density, the one that contributes more to $Z(\beta)$ will be the one with lower \mathcal{O} .

Note that this property works in both directions. In particular, if there exists a process for generating samples of states in \mathcal{S} that satisfy the statistical properties of Eq. (3), then, all else being equal, the samples will more frequently display features that occur most frequently in designs that minimize the objective. In this sense Eq. (3) provides a window into the most important aspects of the design space without needing to know the optimal design.

3. Condensation

It is also instructive to consider the case in which certain regions of the solution space are densely represented in the part of \mathcal{S} for a band of \mathcal{O} .

The first case we will consider is $\mathcal{O}_{\min} \leq \mathcal{O} \leq \mathcal{O}_{\min} + \Delta\mathcal{O}$. For illustrative purposes, for the moment, let's consider constant volume in x_{\perp} over this band of \mathcal{O} , i.e. $\Omega_{\perp}(\mathcal{O}) = \Omega_{\perp}$. We can compute the contribution of such a region to $Z(\beta)$, which will be given by

$$Z(\beta, \Delta\mathcal{O}) = \int_{\mathcal{O}_{\min}}^{\mathcal{O}_{\min} + \Delta\mathcal{O}} d\mathcal{O} e^{-\beta\mathcal{O}} \Omega_{\perp} . \quad (38)$$

One could compute this integral in closed form, but it is more useful not to. Instead, one can use the mean value theorem which dictates that there exists some \mathcal{O}_* that satisfies

$\mathcal{O}_{\min} \leq \mathcal{O}_* \leq \mathcal{O}_{\min} + \Delta\mathcal{O}$ such that

$$Z(\beta, \Delta\mathcal{O}) = \Delta\mathcal{O}\Omega_{\perp} e^{-\beta\mathcal{O}_*}. \quad (39)$$

If Ω_{\perp} is not constant, but satisfies some meaningful notions of continuity, then the same relationship holds, but with Ω_{\perp} replaced by some appropriate notion of a mean.

How should one interpret this?

Suppose, for example, there are certain aspects of the design that characterize all of the possible design choices in which the objective is within $\Delta\mathcal{O}$ of the minimum. That set of design choices will materialize as contributions to $Z(\beta)$ with a strength that is proportional both to the range $\Delta\mathcal{O}$ for which they are common, and the volume Ω_{\perp} of the transverse space they occupy, with a scaling factor that is determined by the objective function and β . Note that because of the exponential dependence of this scaling factor on β , $\mathcal{O}_* \rightarrow \mathcal{O}_{\min}$ as $\beta \rightarrow \infty$.

Now suppose there is a second region of \mathcal{S} that is localized in a region of the transverse space away from \mathcal{O}_{\min} , e.g., $\mathcal{O}_{\text{bad}} \leq \mathcal{O} \leq \mathcal{O}_{\text{bad}} + \Delta\mathcal{O}$. To facilitate comparison, we will take Ω_{\perp} and $\Delta\mathcal{O}$ to be the same as before and $\mathcal{O}_{\text{bad}} - \mathcal{O}_{\min} \gg \Delta\mathcal{O}$. Integrating to find the contribution to $Z(\beta)$ would yield the same expression as Eq. (39) except that now $\mathcal{O}_{\text{bad}} \leq \mathcal{O}_* \leq \mathcal{O}_{\text{bad}} + \Delta\mathcal{O}$. The relative contribution of the two regions to $Z(\beta)$ differs exponentially the value of \mathcal{O}_* . In particular, the ratio of the near minimal contribution to the non-minimal contribution will be $\exp(-\beta(\mathcal{O}_{\text{bad}} - \mathcal{O}_{\min})) = \exp(-(\mathcal{O}_{\text{bad}} - \mathcal{O}_{\min})/T)$.

Overall, suppose one is ignorant not only of \mathcal{O}_{\min} but also the value of χ_{\perp} there, but still able to construct some way of sampling the \mathcal{S}_{β} according to Eq. (3). Regardless of whether this sampling is generated geometrically, statistically, or physically, the predominance of design features that characterize optimal solutions versus those that are that occupy a similar (untransformed) volume of \mathcal{S} will be discernible for temperatures $T \lesssim (\mathcal{O}_{\text{bad}} - \mathcal{O}_{\min})$. In more colloquial terms, common elements that distinguish “bad” solutions from “good” ones (as scored by \mathcal{O}) are culled from the solution space at higher T .

For example, if one was to generate samples on \mathcal{S}_{β} by Markov-chain Monte Carlo, the principle of detailed balance would indicate that if the sampling was ergodic, key features of the design would begin to condense at higher T . Similar effects would exist in other sampling methods. We will not explore this at further length here, but a detailed account of this plays out in practice in the context of structural design can be found in

Ref. [27].

IV. ILLUSTRATIVE EXAMPLE: LINEAR PROGRAMMING

Although we are primarily interested in problems that don't admit closed-form evaluation of the Pareto-Laplace filter, examples that do admit closed-form evaluation are useful for illustrating key properties of $Z(\beta)$. This section presents an example of a two-dimensional linear programming problem. Appendix E considers general linear programming problems and Appendix F considers quadratic programming.

For concreteness, consider the minimization problem:

$$\begin{aligned} \min \mathcal{O} &= -4x_1 - 3x_2 + 36 \\ \text{s.t. } 3x_1 + 6x_2 &\leq 48 \\ 4x_1 + 2x_2 &\leq 32 \\ x_1 + x_2 &\leq 10 \\ x_1 &\geq 0 \\ x_2 &\geq 0 \end{aligned}$$

For ease of illustration, it is useful to exploit the symmetry properties of the framework (see Sec. II C) to make a coordinate transformation

$$x_1 = -\frac{3}{5}x_{\perp} - \frac{4}{25}\mathcal{O} + 6x_2 = \frac{4}{5}x_{\perp} - \frac{3}{25}\mathcal{O} + 4$$

which puts the optimal solution at $(x_{\perp}, \mathcal{O}) = (2, 0)$. The feasible region is a convex polygon with its remaining vertices at $(-\frac{22}{5}, 4)$, $(\frac{14}{5}, 2)$, $(\frac{34}{5}, 12)$, and $(\frac{2}{5}, 36)$. From this we can compute $\Omega_{\perp}(\mathcal{O})$ for each region. We find

$$\Omega_{\perp} = \begin{cases} \frac{5}{2}\mathcal{O} & 0 \leq \mathcal{O} \leq 2 \\ \frac{3}{2}\mathcal{O} + 2 & 2 \leq \mathcal{O} \leq 4 \\ \frac{1}{4}\mathcal{O} + 7 & 4 \leq \mathcal{O} \leq 12 \\ 15 - \frac{5}{12}\mathcal{O} & 12 \leq \mathcal{O} \leq 36 \end{cases}. \quad (40)$$

We can then compute $Z(\beta)$ according to Eq. (3) to get

$$Z(\beta) = \frac{5}{2\beta^2} - \frac{1}{\beta^2}e^{-2\beta} - \frac{5}{4\beta^2}e^{-4\beta} - \frac{2}{3\beta^2}e^{-12\beta} + \frac{5}{12\beta^2}e^{-36\beta}. \quad (41)$$

It is important to make some remarks about the structure of $Z(\beta)$. First, each term has a factor of β^{-2} that traces to the linear dependence of Ω_{\perp} on \mathcal{O} in each of the regions. Second the numerical coefficient is related to the change in the rate of linear dependence in each of the regions. Finally, each term has an exponential dependence that is determined by the value of the objective at each of the basic feasible solutions, i.e., by the vertices of the feasible region.

This latter property, i.e., the existence of a decay mode corresponding to each basic feasible solution is an important property of the transform. In other settings similar features in Laplace transforms correspond to characteristic modes that capture essential behaviours of a system. Here we see that, for linear programming, an analogous property emerges via the vertices of the feasible region.

It is instructive to compute the moments of $Z(\beta)$, and to do this it is convenient to write

$$-\log Z = 2 \log \beta - \log \left(\frac{5}{2} \right) - \log \left(1 - \frac{2}{5} e^{-2\beta} - \frac{1}{2} e^{-4\beta} - \frac{4}{15} e^{-12\beta} + \frac{1}{6} e^{-36\beta} \right). \quad (42)$$

We can then compute $\langle \mathcal{O} \rangle$ as

$$\langle \mathcal{O} \rangle = \frac{2}{\beta} - \frac{\frac{4}{5} e^{-2\beta} + 4 e^{-4\beta} + \frac{48}{15} e^{-12\beta} - 6 e^{-36\beta}}{1 - \frac{2}{5} e^{-2\beta} - \frac{1}{2} e^{-4\beta} - \frac{4}{15} e^{-12\beta} + \frac{1}{6} e^{-36\beta}}. \quad (43)$$

Based on the geometric arguments above, we would expect that $\langle \mathcal{O} \rangle = 0$ as $\beta \rightarrow \infty$, and Eq. (43) clearly satisfies this property.

Our analysis of an example problem in linear programming revealed a particular form for $Z(\beta)$ in Eq. (41) that was determined by the geometric features of the feasible region. We arrived at this result with the assistance of an affine transformation of the feasible region. Though this affine transformation was useful for illustrative purposes, in linear programming problems of interest one should not expect to be able to compute such a transformation without already knowing the solution. However, it is important to note that although the affine transformation we used in the example problem was convenient, it was not necessary. As we showed in Sec. II C, the Pareto-Laplace filter defined in Eq. (3) has well defined properties under coordinate transformations. These transformation properties imply that any means that could generate $Z(\beta)$ in any formulation of the problem will yield a sum of exponentially decaying modes $\exp(-\beta \mathcal{O}_v)$ where \mathcal{O}_v is the objective evaluated at each of the basic feasible solutions that correspond with the vertices of the feasible region.

Several things are interesting to note here. In Appendix E we extend our analysis to \mathcal{S} in which the dimensionality of \mathbf{x}_\perp is larger, and we compute $Z(\beta)$ by integrating piecewise in \mathcal{O} over the polytope that defines the feasible region. Each piecewise region corresponds to a location where a new constraint takes hold because it results in a change in the form of $\Omega_\perp(\mathcal{O})$. This break in the integration induces a factor of $\exp(-\beta\mathcal{O})$ at a vertex (or in some special cases, an edge) of the polytope. This means that (i) geometric features of the solution space imprint themselves on the form of $Z(\beta)$ in a discernible way, and that (ii) the analogue of long-lived transients in time-domain problems are near optimal features in optimization problems.

V. DISCUSSION

Prompted by the challenge of relating the structure of an optimization problem to the structure of its solution, we constructed a Pareto-Laplace integral transformation framework for design problems. We showed that the Pareto-Laplace framework can be viewed from geometric, statistical, and physical perspectives (Fig. 2 illustrates this schematically). This multiplicity of perspectives opens several windows on the relationship between problem- and solution structure in optimization. We computed closed-form, explicit results in some example cases, and showed how to construct a general formulation of the approach for problems with an arbitrary number of objectives and constraints. We also related our framework to other known approaches, some of which can be understood as special cases.

The primary goal of the description we presented here was to establish some basic properties of the framework. Because of the generality of the framework, it is not possible to be exhaustive in describing all of the problems it can be applied to, nor the forms of analysis that could be leveraged. We concentrated our analysis of the Pareto-Laplace framework by elucidating some of its key aspects using its physical representation. We connected this framework to both geometry and information theory, but on both fronts, we only invoked relatively primitive tools. More sophisticated tools could be invoked to develop deeper geometric or statistical connections and understanding. Moreover, because the framework is a Laplace transform and because many disciplines have well-established methodologies for handling and interpreting such transforms, practitioners

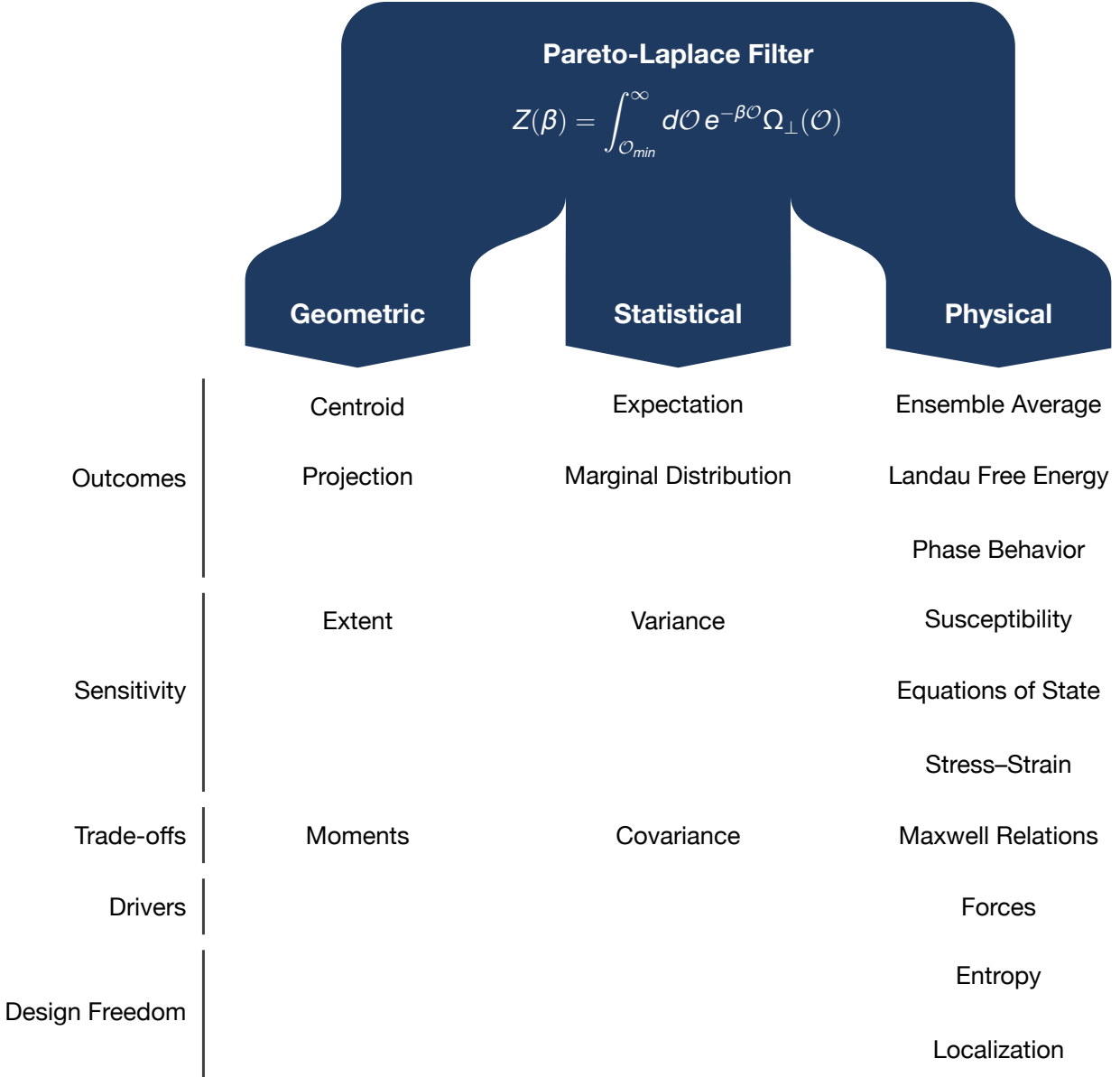


FIG. 2. The Pareto-Laplace filtering framework can be interpreted geometrically, statistically, and physically. This framework provides the means to operationalize multiple different forms of design investigation in terms of one or more of the three perspectives.

may find other fruitful ways of approaching this framework beyond the physics-centric presentation we gave here.

The multiplicity of settings in which this framework can be invoked gives rise to a corresponding multiplicity of means to implement it. We pointed to existing implementations of this framework that leverage Monte Carlo,[11, 14–16] molecular dynamics,[11,

19] and tensor network techniques.[13, 24] However, this list is in no way exhaustive. Moreover, note that the techniques that have already been used to implement the Pareto-Laplace framework were adapted from techniques that were developed to attack other problems, and we believe that the generality of the framework will yield implementations adapted from other existing algorithms.

Finally, we identified a number of existing results in the literature that are examples of the present framework, including examples from the design of self-assembled materials, from naval architecture, from land-use planning, and from structural design. This list is not exhaustive, and we expect to report soon on applications to problem spaces beyond this set.

ACKNOWLEDGMENTS

We acknowledge the support of the Natural Sciences and Engineering Research Council of Canada (NSERC) grants RGPIN-2019-05655 and DGEER-2019-00469.

Appendix A: Weighted Additive Multi-Objective Optimization

Although a feature of the present framework is the ability to address multi-objective problems while remaining agnostic about the relative relation among the objectives, it is instructive to illustrate how address problems in which the relationship among the objectives is fixed.

In situations where there is an overall objective that arises as a linear sum of the objectives, one can write an overall objective

$$\mathcal{O} = \sum_i P_i \mathcal{O}_i, \tag{A1}$$

where the P_i are a set of constants with units of $[\mathcal{O}]/[\mathcal{O}_i]$.

1. Weight Parameterization and Competing Pressures

One can compute $Z(\beta)$ from Eq. (A1) by introducing a parameter β and employing Eq. (3). Note that, in general, this recipe would involve $N_o + 1$ parameters for N_o objectives.

The additional parameter is essentially a free parameter that corresponds to an arbitrary choice of units for \mathcal{O} (the units of β should be the inverse of the units of \mathcal{O}). One could, for example, fix the units of \mathcal{O} to match those of one of the objectives, \mathcal{O}_j , set the corresponding $P_j = 1$, and the remaining P_i would function akin to “currency” conversion factors between the objectives.

We note that factors, which are conventionally referred to as “weights” in optimization, do not actually have the mathematical form of weight either in the present framework or in optimization. In particular, whereas physical weight is an extensive parameter, i.e., a parameters that scale with system size, optimization “weights” are intensive. From the point of view of the present framework, “weights” actually take the form of generalized pressures or chemical potentials in the language of physics. In particular P_i are the mathematical analogues of pressure that quantify a form of competition between objectives. This mathematical form aligns nicely with the notion of “competing pressures” that is invoked in vernacular descriptions of multi-objective problems. Further, note that in these cases $\Omega_{\perp} = \Omega_{\perp}(\mathcal{O}, P_i)$. The P_i dependence arises because the geometry of the Pareto slicing depends on functional form of Ω , which in turn depends on the choice of the competing pressures.

2. Beyond Additive Multi-Objective Problems

What if the overall objective is not a linear combination of the component objectives? Suppose the overall objective involved a product of objectives. In these cases one can introduce a β with units that are the inverse of the units of the product, and then proceed to compute Eq. (3).

Appendix B: Design Space Geometry Effects on Objective Function Moments

Although the limit $\beta \rightarrow \infty$ or $T \rightarrow 0$ filters out all non-optimal solutions, near the strict limit, i.e., for sufficiently large β or sufficiently small T the geometry of the solution space leaves a clear imprint on the moments.

One situation is to understand the temperatures at which sub-leading corrections are important in $\langle \mathcal{O} \rangle (T)$. To this end, consider the case where there is a single minimum at

\mathcal{O}_{\min} and the volume in the vicinity is

$$\Omega_{\perp}(\mathcal{O}) = \gamma(\mathcal{O} - \mathcal{O}_{\min})^{N_{\text{IP}}/\nu-1} \left(1 + \left(\frac{\mathcal{O} - \mathcal{O}_{\min}}{T_*} \right)^{\Delta N} \right), \quad (\text{B1})$$

where the leading order behaviour matches that of Eq. (31) and includes sub-leading order corrections scaled by T_* , which is a constant with the same units as the objective, and ΔN is the change in scaling of Ω as the temperature increases. A volume of states of this form could imply that a distance approximately T_* in the \mathcal{O} direction in \mathcal{S} some additional set of ΔN degrees of freedom become “active”, for example.

Given Ω_{\perp} in the form in Eq. (B1), we can compute the Laplace transform Eq. (3) which gives

$$Z(T) = \gamma \Gamma\left(\frac{N_{\text{IP}}}{\nu}\right) e^{-\mathcal{O}_{\min}/T} T^{N_{\text{IP}}/\nu} \left(1 + \frac{\Gamma\left(\frac{N_{\text{IP}}}{\nu} + \Delta N\right)}{\Gamma\left(\frac{N_{\text{IP}}}{\nu}\right)} \left(\frac{T}{T_*}\right)^{\Delta N} \right). \quad (\text{B2})$$

One could then, for example, compute the effect of Eq. (B1) on \mathcal{O} and find

$$\langle \mathcal{O} \rangle \approx \mathcal{O}_{\min} + \frac{N_{\text{IP}}}{\nu} T + \frac{\Delta N T}{\frac{\Gamma\left(\frac{N_{\text{IP}}}{\nu}\right)}{\Gamma\left(\frac{N_{\text{IP}}}{\nu} + \Delta N\right)} \left(\frac{T_*}{T}\right)^{\Delta N} + 1}. \quad (\text{B3})$$

For $T \ll T_*$, Eq. (B3) recovers the expected form of Eq. (33) near \mathcal{O}_{\min} , i.e.,

$$\langle \mathcal{O} \rangle \approx \mathcal{O}_{\min} + \frac{N_{\text{IP}}}{\nu} T. \quad (\text{B4})$$

For $T \gg T_*$ Eq. (B3) recovers a similar form to Eq. (33) but with $N_{\text{IP}}/\nu \rightarrow N_{\text{IP}}/\nu + \Delta N$ given by

$$\langle \mathcal{O} \rangle \approx \mathcal{O}_{\min} + \left(\frac{N_{\text{IP}}}{\nu} + \Delta N \right) T. \quad (\text{B5})$$

This implies a change in the slope of $\langle \mathcal{O} \rangle$ around T_* , with the slope serving as an indicator of the active degrees of freedom on either side of this transition.

Appendix C: Geodesics: Minimal Length Descent to Objective Minima

For the purpose of interpretation or algorithms, it is useful to consider geodesics on the filtered space. Taking the metric as in Eq. (4) we can parameterize a curve via the objective \mathcal{O} and write the length of a path from $(\mathcal{O}_1, \mathbf{x}_{\perp}^{(1)})$ to $(\mathcal{O}_2, \mathbf{x}_{\perp}^{(2)})$ as

$$L = \int_{\mathcal{O}_1}^{\mathcal{O}_2} d\mathcal{O} \sqrt{1 + e^{-2\beta\mathcal{O}/(N-1)} \left(\frac{d\mathbf{x}_{\perp}}{d\mathcal{O}} \right)^2}, \quad (\text{C1})$$

where we will take that the induced metric in the transverse space is flat, and where we assume that $\mathcal{O}_2 > \mathcal{O}_1$. In this case, we get that

$$\frac{e^{-2\beta\mathcal{O}/(N-1)} \frac{d\vec{x}_\perp}{d\mathcal{O}}}{1 + e^{-2\beta\mathcal{O}/(N-1)} \left(\frac{d\vec{x}_\perp}{d\mathcal{O}}\right)^2} = \vec{v}_\perp \quad (\text{C2})$$

where \vec{v}_\perp is a set of $N - 1$ constants. We can use this to find

$$\frac{d\vec{x}_\perp}{d\mathcal{O}} = \frac{e^{\beta\mathcal{O}/(N-1)} \vec{v}_\perp}{\sqrt{e^{-2\beta\mathcal{O}/(N-1)} - \vec{v}_\perp^2}}, \quad (\text{C3})$$

where

$$|\vec{v}_\perp| < e^{-\beta\mathcal{O}_2/(N-1)}. \quad (\text{C4})$$

Given this restriction, we can re-parameterize \vec{v}_\perp as

$$\vec{v}_\perp = \sin \alpha \hat{e}_\perp e^{-\beta\mathcal{O}_2/(N-1)}, \quad (\text{C5})$$

where \hat{e}_\perp is a unit vector in the transverse space, and α is the angle of inclination for a straight line connecting the two end points in the limit $\beta \rightarrow 0$ (i.e., in the untransformed space). This gives

$$\frac{d\vec{x}_\perp}{d\mathcal{O}} = \frac{\sin \alpha e^{-\beta(\mathcal{O}_2 - \mathcal{O})/(N-1)}}{\sqrt{e^{-2\beta\mathcal{O}/(N-1)} - \sin^2 \alpha e^{-2\beta\mathcal{O}_2/(N-1)}}} \hat{e}_\perp. \quad (\text{C6})$$

It is useful to note that Eq. (C6) implies that $\frac{d\vec{x}_\perp}{d\mathcal{O}}$ grows exponentially in \mathcal{O} . That, in turn, means that a minimal length path between an arbitrary point $(\mathcal{O}', \vec{x}'_\perp)$ in the transformed space and the minimum $(\mathcal{O}_{\min}, \vec{x}_\perp^{\min})$ will converge rapidly in the transverse directions as it descends in \mathcal{O} .

We would like to integrate Eq. (C6), so it is convenient to first rearrange

$$\frac{d\vec{x}_\perp}{d\mathcal{O}} = \hat{e}_\perp e^{\beta\mathcal{O}_2/(N-1)} \frac{e^{-2\beta(\mathcal{O}_2 - \mathcal{O})/(N-1)} \sin \alpha}{\sqrt{1 - e^{-2\beta(\mathcal{O}_2 - \mathcal{O})/(N-1)} \sin^2 \alpha}} \quad (\text{C7})$$

If we define $\Delta x_\perp = (x_\perp^{(2)} - x_\perp^{(1)}) \cdot \hat{e}_\perp$, this gives

$$\Delta x_\perp = e^{\beta\mathcal{O}_2/(N-1)} \int_{\mathcal{O}_1}^{\mathcal{O}_2} d\mathcal{O} \frac{e^{-2\beta(\mathcal{O}_2 - \mathcal{O})/(N-1)} \sin \alpha}{\sqrt{1 - e^{-2\beta(\mathcal{O}_2 - \mathcal{O})/(N-1)} \sin^2 \alpha}}. \quad (\text{C8})$$

It is convenient to make a change of variables

$$\sin \theta = \sin \alpha e^{-\beta(\mathcal{O}_2 - \mathcal{O})/(N-1)}, \quad (\text{C9})$$

which gives

$$\Delta x_{\perp} = \frac{N-1}{\beta} \frac{e^{\beta \mathcal{O}_2 / (N-1)}}{\sin \alpha} \int_{\sin^{-1}(\sin \alpha e^{-\beta \Delta \mathcal{O} / (N-1)})}^{\alpha} d\theta \sin \theta, \quad (\text{C10})$$

where $\Delta \mathcal{O} = \mathcal{O}_2 - \mathcal{O}_1$. Eq. (C10) relates the transverse displacement with respect to the change in the objective to an effective change in an arc length imposed by the geometric filter. Integrating this gives

$$\Delta x_{\perp} = \frac{N-1}{\beta} \frac{e^{\beta \mathcal{O}_2 / (N-1)}}{\sin \alpha} \left(\sqrt{1 - e^{-2\beta \Delta \mathcal{O} / (N-1)} \sin^2 \alpha} - \cos \alpha \right). \quad (\text{C11})$$

In essence Eq. (C11) is akin to a ‘‘line of sight’’ correction to the inclination angle α between $(\mathcal{O}_1, x_{\perp}^{(1)})$ and $(\mathcal{O}_2, x_{\perp}^{(2)})$ that is imposed by the spatial curvature of the filter in \mathcal{S}_{β} .

Appendix D: Example: Manifestations of Multiple Minima

This feature is clear in the linear programming example we showed above, but it is useful to consider how similar behaviours could emerge in non-convex problems. To give a sample illustration of this, we will consider a simple problem that represents the existence of multiple minima.

Suppose that there are two minima $\mathcal{O}_{\min}^{(G,L)}$, where we are assuming one is a local minimum and the other is a global minimum such that $\mathcal{O}_{\min}^{(G)} < \mathcal{O}_{\min}^{(L)}$, and that there are volumes associated with each that have the form

$$\Omega_{\perp}(\mathcal{O}) = \gamma_G \theta(\mathcal{O} - \mathcal{O}_{\min}^{(G)}) (\mathcal{O} - \mathcal{O}_{\min}^{(G)})^{N_{\text{IP}}^{(G)}/\nu - 1} + \gamma_L \theta(\mathcal{O} - \mathcal{O}_{\min}^{(L)}) (\mathcal{O} - \mathcal{O}_{\min}^{(L)})^{N_{\text{IP}}^{(L)}/\nu - 1}, \quad (\text{D1})$$

where $\gamma_{G,L}$ are constant coefficients, $\theta(\cdot)$ is the unit step function which ensure the solution space volume contributions vanish below the compliance minima, and $N_{\text{IP}}^{(G,L)}$ are the effective dimensions near the respective minima. From this we can compute the Laplace transform

$$Z(\beta) = \gamma_G \Gamma\left(\frac{N_{\text{IP}}^{(G)}}{\nu}\right) e^{-\beta \mathcal{O}_{\min}^{(G)}} \beta^{-N_{\text{IP}}^{(G)}/\nu} + \gamma_L \Gamma\left(\frac{N_{\text{IP}}^{(L)}}{\nu}\right) e^{-\beta \mathcal{O}_{\min}^{(L)}} \beta^{-N_{\text{IP}}^{(L)}/\nu}. \quad (\text{D2})$$

where $\Gamma(\cdot)$ is the gamma function. In terms of T this takes the form

$$Z(T) = \gamma_G \Gamma\left(\frac{N_{\text{IP}}^{(G)}}{\nu}\right) e^{-\beta \mathcal{O}_{\min}^{(G)}} T^{N_{\text{IP}}^{(G)}/\nu} + \gamma_L \Gamma\left(\frac{N_{\text{IP}}^{(L)}}{\nu}\right) e^{-\beta \mathcal{O}_{\min}^{(L)}} T^{N_{\text{IP}}^{(L)}/\nu}. \quad (\text{D3})$$

Both of these forms illustrate that both minima leave their fingerprints as modes in $Z(\beta)$ or $Z(T)$. If we rewrite Eq. (D3) as

$$Z(T) = \gamma_G \Gamma \left(\frac{N_{IP}^{(G)}}{\nu} \right) e^{-\mathcal{O}_{\min}^{(G)}/T} T^{N_{IP}^{(G)}/\nu} \left(1 + \frac{\gamma_L}{\gamma_G} \frac{\Gamma \left(\frac{N_{IP}^{(L)}}{\nu} \right)}{\Gamma \left(\frac{N_{IP}^{(G)}}{\nu} \right)} e^{-(\mathcal{O}_{\min}^{(L)} - \mathcal{O}_{\min}^{(G)})/T} T^{(N_{IP}^{(L)} - N_{IP}^{(G)})/\nu} \right). \quad (D4)$$

we can see that the leading behaviour for small T comes from the global minimum, and that the effects of the local minimum on $Z(T)$ are suppressed by the exponential factor $\exp(-(\mathcal{O}_{\min}^{(L)} - \mathcal{O}_{\min}^{(G)})/T)$. Fig. 3 gives an illustration of this phenomenon.

Note that it is possible to estimate the temperature at which $Z(T)$ goes from being effectively characterized by a single minimum to being characterized by two, which will occur for $T = T_{\times}$ such that

$$e^{-(\mathcal{O}_{\min}^{(L)} - \mathcal{O}_{\min}^{(G)})/T_{\times}} T_{\times}^{(N_{IP}^{(L)} - N_{IP}^{(G)})/\nu} \approx \frac{\gamma_G}{\gamma_L} \frac{\Gamma \left(\frac{N_{IP}^{(G)}}{\nu} \right)}{\Gamma \left(\frac{N_{IP}^{(L)}}{\nu} \right)}. \quad (D5)$$

If the geometry near the two minima is similar, i.e., $N_{IP}^{(L)} \approx N_{IP}^{(G)}$ and $\gamma_L \approx \gamma_G$, then the crossover temperature is given by

$$T_{\times} \approx \mathcal{O}_{\min}^{(L)} - \mathcal{O}_{\min}^{(G)}, \quad (D6)$$

i.e. the objective difference of the two minima. This crossover temperature will change if the growth of states away from the minima is much more rapid for one minimum than the other. It is straightforward to extend the analysis above to any number of minima.

Appendix E: Example: General Linear Programming

In the text, we gave examples of the behaviour of Eq. (3) for some specific examples of linear programming. To further illustrate the behaviour of $Z(\beta)$ in this section we consider a general linear programming problem in \mathbb{R}^n .

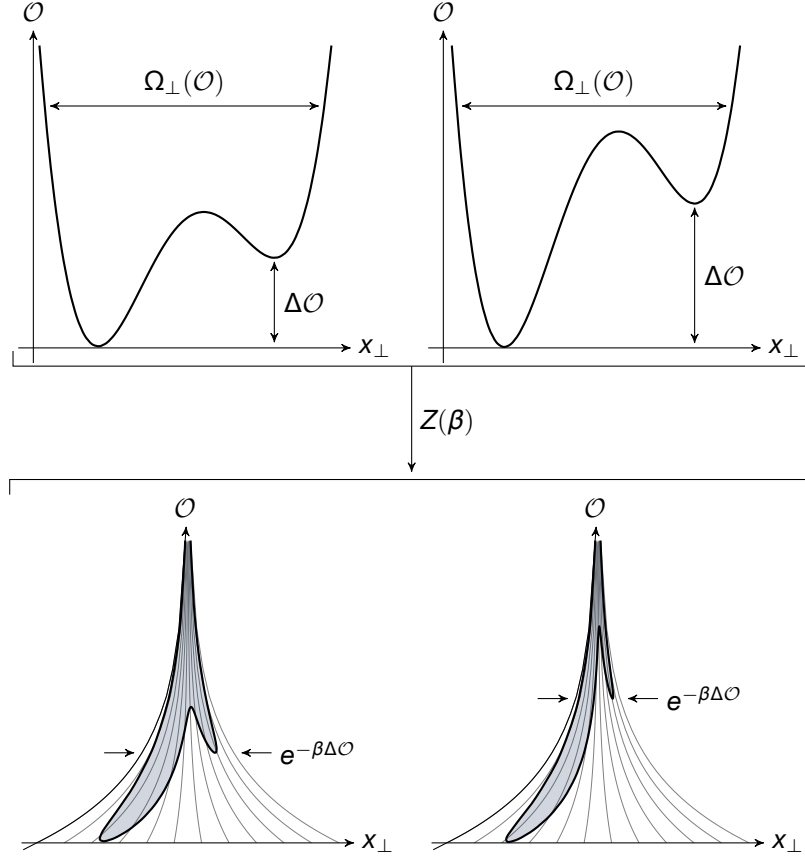


FIG. 3. Schematic representation of Pareto-Laplace transform for a situation with multiple minima. In the pre-filtered picture (top panels), the sub-leading, local minimum is at a lower value of \mathcal{O} in the scenario depicted in the left image compared to the scenario in the right image. In the post-filtered picture (lower panels) the filter more strongly “pinches” the region of the solution space near the local minimum with larger \mathcal{O} (right) compared to the one with lower \mathcal{O} (left), illustrating the essence of the effect anticipated from Eq. (D2).

1. Pareto-Laplace Filter

The general formulation of a linear programming problem with m linear constraints is as Eq. (E1).

$$\begin{aligned}
 \min_{x \in \mathbb{R}^n} \quad & \mathcal{O} = c^\top x + d_0 \\
 \text{s.t.} \quad & h_j^\top x + d_j \leq 0 \quad j = 1, \dots, m
 \end{aligned} \tag{E1}$$

The feasible region, \mathcal{S} , in linear programming, is a polytope made by the intersection of constraints where each is a hyperplane. The problem is to minimize the affine func-

tion $\mathcal{O}(x)$ over this polytope. Given the fact that the objective function is linear, one can translate and rotate the coordinate such that the problem is reparametrized as Eq. (E2).

$$\begin{aligned} \min_{x_{\perp} \in \mathbf{R}^{n-1}} \quad & \mathcal{O} \\ \text{s.t.} \quad & \tilde{\mathbf{h}}_j^{\top} x_{\perp} + h_0 \mathcal{O} + \tilde{\mathbf{d}}_j \leq 0 \quad j = 1, \dots, m \end{aligned} \quad (\text{E2})$$

Without loss of generality, we assume the polytope \mathcal{S} has no edge parallel to the x_{\perp} -plane and N vertices. The vertices of the polytope \mathcal{S} can be found by solving constraint equations. Defining Γ_{η} as the \mathcal{O} -component of η^{th} vertex, the solution space $\Omega_{\perp}(\mathcal{O})$ is a piecewise function like Eq. (E3).

$$\Omega_{\perp}(\mathcal{O}) = \begin{cases} \sum_{i=0}^{n-1} \mathbf{a}_i^{N-1} \mathcal{O}^i & \Gamma_{N-1} \leq \mathcal{O} \leq \Gamma_N \\ \vdots & \vdots \\ \sum_{i=0}^{n-1} \mathbf{a}_i^1 \mathcal{O}^i & \Gamma_1 \leq \mathcal{O} \leq \Gamma_2 \end{cases} \quad (\text{E3})$$

Now, we can find the partition function of the problem as follows according to the definition given in Eq. (3).

$$\begin{aligned} Z(\beta) &= \sum_{\eta=1}^{N-1} \int_{\Gamma_{\eta}}^{\Gamma_{\eta+1}} d\mathcal{O} e^{-\beta \mathcal{O}} \left(\sum_{i=0}^{n-1} \mathbf{a}_i^{\eta} \mathcal{O}^i \right) \\ &= \sum_{\eta=1}^{N-1} \mathcal{F}(\Gamma_{\eta}, \mathbf{a}^{\eta}) e^{-\beta \Gamma_{\eta}} - \mathcal{F}(\Gamma_{\eta+1}, \mathbf{a}^{\eta}) e^{-\beta \Gamma_{\eta+1}} \\ &= \mathcal{F}(\Gamma_1, \mathbf{a}^1) e^{-\beta \Gamma_1} \\ &\quad + \sum_{\eta=2}^{N-1} [\mathcal{F}(\Gamma_{\eta}, \mathbf{a}^{\eta}) - \mathcal{F}(\Gamma_{\eta}, \mathbf{a}^{\eta-1})] e^{-\beta \Gamma_{\eta}} \\ &\quad + \mathcal{F}(\Gamma_N, \mathbf{a}^{N-1}) e^{-\beta \Gamma_N} \end{aligned} \quad (\text{E4})$$

where

$$\mathcal{F}(\Gamma, \mathbf{a}) = \sum_{j=0}^{n-1} \frac{1}{\beta^{j+1}} \frac{d^j}{d\Gamma^j} \left(\sum_{i=0}^{n-1} \mathbf{a}_i \Gamma^i \right)$$

Due to the continuity of $\Omega_{\perp}(\mathcal{O})$, we must have

$$\sum_{i=0}^{n-1} \mathbf{a}_i^{\eta} \Gamma_{\eta+1}^i = \sum_{i=0}^{n-1} \mathbf{a}_i^{\eta+1} \Gamma_{\eta+1}^i$$

This gives,

$$\mathcal{F}(\Gamma_{\eta}, \mathbf{a}^{\eta}) - \mathcal{F}(\Gamma_{\eta}, \mathbf{a}^{\eta-1}) = \sum_{j=1}^{n-1} \frac{1}{\beta^{j+1}} \frac{d^j}{d\Gamma^j} \left(\sum_{i=0}^{n-1} (\mathbf{a}_i^{\eta} - \mathbf{a}_i^{\eta-1}) \Gamma_{\eta}^i \right)$$

Moreover, since $\Omega_{\perp}(\mathcal{O})$ between $\Gamma_{\eta} \leq \mathcal{O} \leq \Gamma_{\eta+1}$ is proportional to $(\mathcal{O} - \Gamma_{\eta})^{n-1}$ for $\eta = 1$ and $\eta = N - 1$,

$$\frac{d^j}{d\Gamma^j} \left(\sum_{i=0}^{n-1} a_i^{\eta} \Gamma_{\eta}^i \right) = 0$$

for all $j \neq n - 1$. Putting all of these together, we can simplify Eq. (E4) as Eq. (E5).

$$Z(\beta) = \sum_{\eta=1}^N \zeta_{\eta} e^{-\beta \Gamma_{\eta}} \quad (\text{E5})$$

where

$$\begin{aligned} \zeta_1 &= \frac{(n-1)!}{\beta^n} a_{n-1}^1 \\ \zeta_{\eta} &= \sum_{j=1}^{n-1} \frac{1}{\beta^{j+1}} \frac{d^j}{d\Gamma^j} \left(\sum_{i=0}^{n-1} (a_i^{\eta} - a_i^{\eta-1}) \Gamma_{\eta}^i \right); \quad 2 \leq \eta \leq N-1 \\ \zeta_N &= -\frac{(n-1)!}{\beta^n} a_{n-1}^{N-1} \end{aligned}$$

2. Invariance

According to the definition of ζ_{η} , the partition function, Z has no 0th order coefficients, a_0^{η} , for any η . This means any translation of the coordinate along x_{\perp} does not change the partition function. Moreover, since only the difference of the 1st order coefficients, $a_1^{\eta} - a_1^{\eta-1}$, exists, any rotation of the coordinate around \mathcal{O} -axis does not change the partition function.

$$x_{\perp} \rightarrow R_{\mathcal{O}} x_{\perp} + \Delta x_{\perp} \quad \Rightarrow \quad Z(\beta) \rightarrow Z(\beta)$$

Although the translation of the coordinate by $\Delta \mathcal{O}$ along \mathcal{O} -axis does not change the geometry of \mathcal{S} , i.e. ζ_{η} will be the same for all η , it changes the Γ_{η} to $\Gamma_{\eta} - \Delta \mathcal{O}$.

$$\mathcal{O} \rightarrow \mathcal{O} + \Delta \mathcal{O} \quad \Rightarrow \quad Z \rightarrow e^{\beta \Delta \mathcal{O}} Z(\beta)$$

3. Numerical Example: Three Dimensions

For concreteness, we give a specific example in three dimensions. Consider the following problem,

$$\begin{aligned} \min \mathcal{O} &= 3x_1 + 4x_2 - 12x_3 \\ \text{s.t. } 5x_1 + 7x_2 + 7x_3 &\leq 19 \\ x_1 - x_3 &\geq 0 \\ x_2 - x_3 &\geq 0 \\ x_3 &\geq 0. \end{aligned}$$

For the matter of illustration, it is useful to make a coordinate transformation such that $\mathcal{O} = \mathcal{O}(x_3)$, and $x_* = (0, 0, 0)$, where x_* is the global optimal point. To do this, we should rotate the coordinate by $\theta = \arccos\left(\frac{\vec{n} \cdot \vec{x}_3}{\|\vec{n}\|\|\vec{x}_3\|}\right)$ around vector $\vec{r}' = \vec{n} \times \vec{x}_3$, where \vec{n} is the normal vector of plane \mathcal{O} . This can be effected by the transformation:

$$\begin{aligned} x &= \frac{4x_1}{13} - \frac{12x_2}{13} + \frac{3x_3}{13} + 1, \\ y &= -\frac{12x_1}{13} - \frac{3x_2}{13} + \frac{4x_3}{13} + 1, \\ z &= -\frac{3x_1}{13} - \frac{4x_2}{13} - \frac{12x_3}{13} + 1. \end{aligned}$$

The transformed objective function is $\mathcal{O} = 13z - 5$. Thus, we should set $z = \frac{1}{13}(\mathcal{O} + 5)$. Then the optimization problem becomes

$$\begin{aligned} \min \quad & \mathcal{O} \\ \text{s.t. } \quad & \frac{1}{13} \left(-\frac{41}{13}(\mathcal{O} + 5) - 85x - 109y \right) \leq 0 \\ & \frac{1}{13} \left(\frac{15(\mathcal{O} + 5)}{13} + 7x - 8y \right) \geq 0 \\ & \frac{1}{13} \left(\frac{16(\mathcal{O} + 5)}{13} - 9x + y \right) \geq 0 \\ & \frac{1}{169}(-12\mathcal{O} - 39x - 52y + 109) \geq 0. \end{aligned}$$

Here $\vec{x}_\perp = (x, y)$. To find Ω_\perp , we need to find the equations of the lines that define the polygon that defines the boundary of the feasible region in the (x, y) -plane. There are four constraints and the intersection of each pair of them gives a line. One can find the

following line equations for this problem,

$$\begin{aligned}
l_1(\mathcal{O}) &: \left\{ x = -\frac{151\mathcal{O}}{1443} - \frac{755}{1443}, y = \frac{76\mathcal{O}}{1443} + \frac{380}{1443} \right\} \\
l_2(\mathcal{O}) &: \left\{ x = \frac{131\mathcal{O}}{1066} + \frac{655}{1066}, y = -\frac{133\mathcal{O}}{1066} - \frac{665}{1066} \right\} \\
l_3(\mathcal{O}) &: \left\{ x = \frac{88\mathcal{O}}{13} - \frac{977}{13}, y = \frac{76\mathcal{O}}{13} - \frac{69\mathcal{O}}{13} \right\} \\
l_4(\mathcal{O}) &: \left\{ x = \frac{11\mathcal{O}}{65} + \frac{11}{13}, y = \frac{19\mathcal{O}}{65} + \frac{19}{13} \right\} \\
l_5(\mathcal{O}) &: \left\{ x = \frac{11}{13} - \frac{3\mathcal{O}}{13}, y = \frac{19}{13} - \frac{3\mathcal{O}}{52} \right\} \\
l_6(\mathcal{O}) &: \left\{ x = \frac{4\mathcal{O}}{39} + \frac{11}{13}, y = \frac{19}{13} - \frac{4\mathcal{O}}{13} \right\}
\end{aligned}$$

These lines intersect at the vertices of the feasible region for each \mathcal{O} . For instance, the intersection of l_1 and l_2 gives the K : $(0, 0, -5)$. Thus, $\Gamma_1 = -5$

$$\begin{aligned}
\Gamma_1 &= -5 \\
\Gamma_2 &= 0 \\
\Gamma_3 &= \frac{76}{7} \\
\Gamma_4 &= \frac{57}{5}.
\end{aligned}$$

Between Γ_1 and Γ_2 , for each \mathcal{O} , Ω_{\perp} is the area of a triangle bounded by l_1 , l_2 , and l_4 . Defining \vec{e}_{ij} as the vector starts on l_i and ends on l_j lines for the same \mathcal{O} , we can find the area of the triangle as $\frac{1}{2}|\vec{e}_{12} \times \vec{e}_{14}|$. In the same way, between Γ_2 and Γ_3 , and between Γ_3 and Γ_4 , Ω_{\perp} is the area of a trapezoid, and a triangle, with area of $\frac{1}{2}|\vec{e}_{16} \times \vec{e}_{25}|$, and $\frac{1}{2}|\vec{e}_{26} \times \vec{e}_{23}|$, respectively. Finally, the Ω_{\perp} is as Eq. E6.

$$\Omega_{\perp} = \begin{cases} \frac{4693(\mathcal{O}+5)^2}{91020} & -5 \leq \mathcal{O} \leq 0 \\ -\frac{689\mathcal{O}^2}{12136} + \frac{4693\mathcal{O}}{9102} + \frac{23465}{18204} & 0 \leq \mathcal{O} \leq \frac{76}{7} \\ \frac{13}{492}(57 - 5\mathcal{O})^2 & \frac{76}{7} \leq \mathcal{O} \leq \frac{57}{5} \end{cases}. \quad (\text{E6})$$

Then using Eq.(E5), we have

$$Z(\beta) = \frac{1}{\beta^3} \frac{4693}{45510} e^{5\beta} - \frac{1}{\beta^3} \frac{13}{60} + \frac{1}{\beta^3} \frac{637}{444} e^{-(76/7)\beta} - \frac{1}{\beta^3} \frac{325}{246} e^{-(57/5)\beta}. \quad (\text{E7})$$

Note that in this form, $Z(\beta)$ has four modes with exponential dependence on β according to \mathcal{O} evaluated at each basic feasible solution, i.e. each vertex of the polyhedron bounding the feasible region. The exponent of the polynomial coefficient, β^{-3} , corresponds to

the dimensionality of the problem, and there is a numerical factor determined by the geometry of the feasible region between basic feasible solutions.

Appendix F: Example: Quadratic Problems

1. Simple Case

Although evaluating Eq. (3) for most nonlinear problems could leverage numerical techniques such as Monte Carlo, molecular dynamics, or tensor network methods, it may be instructive to consider a case in which it can be computed exactly.

Consider a case where $\mathcal{S} = \{(x_1, x_2) | x_{1,2} \in \mathbb{R}\}$, $\mathcal{O} = (x_1^2 + x_2^2)$, and

$$\Omega_{\perp}(\mathcal{O}) = \int_{-\infty}^{\infty} dx_1 \int_{-\infty}^{\infty} dx_2 \delta(\mathcal{O} - (x_1^2 + x_2^2)) . \quad (\text{F1})$$

If we make the change of variables

$$x_1 = r \cos \theta \quad x_2 = r \sin \theta , \quad (\text{F2})$$

we have that the volume of the solution space transverse to the objective at some particular \mathcal{O} is

$$\Omega_{\perp}(\mathcal{O}) = \int_0^{2\pi} d\theta \int_0^{\infty} dr r \delta(\mathcal{O} - r^2) . \quad (\text{F3})$$

Using the delta-function identity

$$\delta(\mathcal{O} - r^2) = \frac{\delta(r - \sqrt{\mathcal{O}})}{2\sqrt{\mathcal{O}}} , \quad (\text{F4})$$

yields

$$\Omega_{\perp}(\mathcal{O}) = \pi . \quad (\text{F5})$$

We get then that

$$Z(\beta) = \frac{\pi}{\beta} . \quad (\text{F6})$$

Note that this form gives $Z(\beta)$ as a single mode with the value of the objective function taking the value of 0 at the minimum, π is clearly a geometric coefficient that describes the growth of the solution space with the objective, and $Z(\beta) \propto (\beta)^{-1}$ because volume of the transverse space is constant.

2. General Quadratic Programming

Consider a more general quadratic program in \mathbb{R}^N with an objective function of the form

$$\mathcal{O} = \frac{1}{2} \mathbf{x}^T \mathbf{A} \mathbf{x} - \mathbf{b}^T \mathbf{x}, \quad (\text{F7})$$

where \mathbf{A} is a symmetric, positive definite matrix, and $\mathbf{b} \in \mathbb{R}^N$. In this case Eq. (3) gives

$$Z(\beta) = \int d^N \mathbf{x} e^{-\beta(\frac{1}{2} \mathbf{x}^T \mathbf{A} \mathbf{x} - \mathbf{b}^T \mathbf{x})}. \quad (\text{F8})$$

a. Evaluating the Transform

To evaluate this, we make a change of variables

$$\mathbf{x} = \mathbf{y} + \mathbf{A}^{-1} \mathbf{b}, \quad (\text{F9})$$

which gives $Z(\beta)$ as

$$Z(\beta) = e^{-\frac{\beta}{2} \mathbf{b}^T \mathbf{A}^{-1} \mathbf{b}} \int d^N \mathbf{y} e^{-\frac{\beta}{2} \mathbf{y}^T \mathbf{A} \mathbf{y}}. \quad (\text{F10})$$

Standard formulae (see, e.g., Ref. [30]) then give

$$Z(\beta) = \left(\frac{2\pi}{\beta} \right)^{N/2} \det(\mathbf{A})^{-1/2} e^{-\frac{\beta}{2} \mathbf{b}^T \mathbf{A}^{-1} \mathbf{b}}. \quad (\text{F11})$$

If we suppose that there is a set of unit eigenvectors

$$\mathbf{A} \hat{\lambda}_i = \lambda_i \hat{\lambda}_i, \quad (\text{F12})$$

and we take

$$\mathbf{b} = \sum_i b_i \hat{\lambda}_i, \quad (\text{F13})$$

then Eq. (F11) takes the form

$$Z(\beta) = \left(\frac{2\pi}{\beta} \right)^{N/2} \left(\prod_i \lambda_i^{-1/2} \right) e^{-\frac{\beta}{2} \sum_i \frac{b_i^2}{\lambda_i}}. \quad (\text{F14})$$

We can interpret this quantity as follows. Since the problem is globally convex, there is a single mode, that corresponds to the global minimum. The growth of solutions around the minimum is determined by the dimensionality of the problem (N) and the spectrum of \mathbf{A} (via λ_i). The weight of the mode is also determined by the spectrum (again via λ_i), and by the location of the global minimum (via b_i).

b. Near-Optimal Behaviour

Given $Z(\beta)$ in Eq. (F14) one can consider the near optimal behaviour of the objective \mathcal{O} . We can deduce the near optimal behaviour via Eq. (22), which gives

$$\langle \mathcal{O} \rangle = \frac{1}{2} \mathbf{b}^\top \mathbf{A}^{-1} \mathbf{b} + \frac{1}{2} \mathbf{N} \mathbf{T}, \quad (\text{F15})$$

where we have used $\mathbf{T} = 1/\beta$. Note that the temperature dependence is an example of what is referred to in physics as the equipartition theorem (see, e.g., Ref. [28]).

c. Transverse Geometry

We evaluated Eqs. (3) and (22) without the need to decompose \mathcal{S} to explicitly determine Ω_\perp . However, it may be instructive to show how to effect the decomposition. In particular, it is useful to understand the origin of the ν factor in various scaling relations.

The transverse volume is given by

$$\Omega_\perp(\mathcal{O}) = \int d^N \mathbf{x} \delta \left(\mathcal{O} - \frac{1}{2} \mathbf{x}^\top \mathbf{A} \mathbf{x} + \mathbf{b}^\top \mathbf{x} \right). \quad (\text{F16})$$

We first make the change of variables in Eq. (F9) which gives

$$\Omega_\perp(\mathcal{O}) = \int d^N \mathbf{y} \delta \left(\mathcal{O} - \frac{1}{2} \mathbf{y}^\top \mathbf{A} \mathbf{y} \right). \quad (\text{F17})$$

We will assume that \mathbf{A} can be diagonalized by a similarity transformation in $\mathbf{Q} \in \text{SO}(N)$, and make another change of variables $\mathbf{u} = \mathbf{Q} \mathbf{y}$, which gives

$$\Omega_\perp(\mathcal{O}) = \int d^N \mathbf{u} \delta \left(\mathcal{O} - \frac{1}{2} \mathbf{u}^\top \boldsymbol{\Lambda} \mathbf{u} \right), \quad (\text{F18})$$

where $\boldsymbol{\Lambda}$ is a diagonal matrix of the eigenvalues of \mathbf{A} . We then make yet another change of variables by defining $\mathbf{v} \in \mathbb{R}^N$, such that

$$v_i = \sqrt{\frac{\lambda_i}{2}} u_i, \quad (\text{F19})$$

which gives

$$\Omega_\perp(\mathcal{O}) = \frac{2^{N/2}}{\det(\mathbf{A})^{1/2}} \int d^N \mathbf{v} \delta(\mathcal{O} - \mathbf{v}^2). \quad (\text{F20})$$

We make a final change of variables to polar coordinates to get

$$\Omega_\perp(\mathcal{O}) = \frac{2^{N/2}}{\det(\mathbf{A})^{1/2}} \int d\omega_{N-1} \int dr r^{N-1} \delta(\mathcal{O} - r^2), \quad (\text{F21})$$

where $r^2 = v^2$, and $d\omega$ is the volume measure for the solid angle. We can then apply the identity in Eq. (F4), to get

$$\Omega_{\perp}(\mathcal{O}) = \frac{2^{N/2}}{\det(\mathbf{A})^{1/2}} \int d\omega_{N-1} \int dr r^{N-1} \frac{\delta(r - \sqrt{\mathcal{O}})}{2\sqrt{\mathcal{O}}} . \quad (\text{F22})$$

Using the fact that

$$\int d\omega_{N-1} = \frac{2\pi^{N/2}}{\Gamma\left(\frac{N}{2}\right)} , \quad (\text{F23})$$

we get that

$$\Omega_{\perp}(\mathcal{O}) = \frac{(2\pi)^{N/2}}{\det(\mathbf{A})^{1/2} \Gamma\left(\frac{N}{2}\right)} \mathcal{O}^{\frac{N}{2}-1} . \quad (\text{F24})$$

If one inserts this form into Eq. (3) and notes that

$$\mathcal{O}_{\min} = \frac{1}{2} \mathbf{b}^T \mathbf{A} \mathbf{b} \quad (\text{F25})$$

then one recovers Eq. (F14).

Note that compared with the analysis of the general linear program in Appendix E, the for the quadratic program here the difference in the scaling v arises from the difference in parametric dependence of the objective function on the design variables x .

Appendix G: Example: Non-Analytic Volume–Objective Problem

We gave detailed analyses of cases in which the volume of Pareto-slices of solution space depend analytically on the objective function. There may be cases in which the Pareto-slice volume is a continuous function of the objective, but it does not have continuous derivatives. Here, examine an example case in which $\Omega_{\perp}(\mathcal{O})$ is defined piecewise.

Consider the case where some sector of \mathcal{S} is “in play” near the minimum, up to some saturation point, \mathcal{O}_* , in \mathcal{O} , after which a different set of degrees of freedom comes into play. We represent this by

$$\Omega_{\perp}(\mathcal{O}) = \begin{cases} \gamma_{<} (\mathcal{O} - \mathcal{O}_{\min})^{N_{<}/v_{<} - 1} & \mathcal{O} < \mathcal{O}_* \\ \gamma_{<} (\mathcal{O}_* - \mathcal{O}_{\min})^{N_{<}/v_{<} - 1} + \gamma_{>} (\mathcal{O} - \mathcal{O}_*)^{N_{>}/v_{>} - 1} & \mathcal{O} > \mathcal{O}_* \end{cases} , \quad (\text{G1})$$

where $\gamma_{<,>}$ are geometric coefficients, and $N_{<,>}$ are scaling exponents giving the number of effective degrees of freedom for Ω_{\perp} on either side of \mathcal{O}_* , and $v_{<,>}$ index the growth in \mathcal{O} (e.g., linear, quadratic, etc.).

Integrating Eq. (G1) gives

$$Z(\beta) = e^{-\beta \mathcal{O}_{\min}} \beta^{N_{<}/\nu_{<}} \gamma_{<} (\Gamma(N_{<}/\nu_{<}) - \Gamma(N_{<}/\nu_{<}, \beta(\mathcal{O}_* - \mathcal{O}_{\min})) + e^{-\beta \mathcal{O}_*} \beta^{N_{>}/\nu_{>}} (\gamma_{>} \Gamma(N_{>}/\nu_{>}) + \gamma_{<} [\beta(\mathcal{O}_* - \mathcal{O}_{\min})]^{N_{>}/\nu_{>}}) . \quad (\text{G2})$$

where $\Gamma(\cdot, \cdot)$ is the incomplete Gamma function.

We can use this to find that for $\beta(\mathcal{O}_* - \mathcal{O}_{\min}) \gg 1$ (equivalently $T \ll \mathcal{O}_* - \mathcal{O}_{\min}$)

$$\langle \mathcal{O} \rangle \approx \mathcal{O}_{\min} + \frac{N_{<}}{\nu_{<} \beta} = \mathcal{O}_{\min} + \frac{N_{<} T}{\nu_{<}} , \quad (\text{G3})$$

whereas for $\beta(\mathcal{O}_* - \mathcal{O}_{\min}) \ll 1$ (equivalently $T \gg \mathcal{O}_* - \mathcal{O}_{\min}$)

$$\langle \mathcal{O} \rangle \approx \mathcal{O}_* + \frac{N_{>}}{\nu_{>} \beta} = \mathcal{O}_* + \frac{N_{>} T}{\nu_{>}} . \quad (\text{G4})$$

Note that for $T \ll \mathcal{O}_* - \mathcal{O}_{\min}$ and $T \gg \mathcal{O}_* - \mathcal{O}_{\min}$, \mathcal{O} asymptotes to linear response in T . In both cases, the slope is determined by the power law growth of Ω_{\perp} . The exponent in this power law growth is, in turn, determined by the number of degrees of freedom that are “in play” (i.e., whose variation is subject to filtering) at that level of T (or β).

Appendix H: Special Case: Simulated Annealing

We gave explicit results in a set of problems that could be done in closed form. However, the vast majority of problems of interest do not admit closed-form solutions. We have applied the Pareto-Laplace framework in several cases, which we have described elsewhere, e.g., Refs. [11, 14–16, 18, 19, 21–23]. However, the approach taken in those works differs somewhat with some conventional optimization approaches, so it is instructive to establish a more concrete connection with other approaches.

In this appendix we will describe the relationship of this approach to simulated annealing. Simulated annealing is the optimization approach that shares the closest kinship with the Pareto-Laplace framework. The great utility of simulated annealing for a range of problems led the extension of the original method described in Ref. [10] in a large number of ways. It is not possible to describe each of them here, so we will concentrate on conventional simulated annealing, and we will leave the discussion of extensions to other work.

In the language of the Pareto-Laplace framework, conventional simulated annealing generates a random walk on \mathcal{S}_{β} , where β is “slowly” (in some sense that is determined

by the landscape of the problem) increased from $\beta = 0$ to $\beta \rightarrow \infty$. This protocol tends to converge to the global minimum of the optimization problem, in the Pareto-Laplace framework, because increasing β effectively “sucks the air” out of \mathcal{S}_β for large \mathcal{O} . For large but finite β the remaining finite volume of \mathcal{S}_β is concentrated around \mathcal{O}_{\min} .

The Pareto-Laplace framework adds several elements to simulated annealing. Some of these elements are: (1) The framework is agnostic about processes that occur on \mathcal{S}_β . (2) The aim of the framework is to characterize the entirety of the structure of \mathcal{S}_β , and its various parametric dependencies, rather than focusing on determining optima. (3) The framework adds additional tools, e.g., modes, moments, etc., that aid in the interpretation of optimization results. (4) The framework seeks to situate optimization problems in broader geometric, statistical, and physical context for the purpose of opening up opportunities for the use of tools from those domains of knowledge.

Appendix I: Near-Optimal Scaling

Here we derive the scaling of Ω_\perp in the vicinity of a minimum of arbitrary index ν . We assume that we are interested in $\mathcal{O} - \mathcal{O}_{\min} \approx 0$ so that we can approximate \mathcal{S}_β locally as $\mathbb{R}^{N_{\text{IP}}}$ near the minimum, which we take to be at x_0 .

In this setting we have that

$$\Omega_\perp(\mathcal{O}) = \int d^{N_{\text{IP}}}x \delta(\mathcal{O} - |x - x_0|^\nu). \quad (\text{I1})$$

Defining $y = x - x_0$ gives

$$\Omega_\perp(\mathcal{O}) = \int d^{N_{\text{IP}}}y \delta(\mathcal{O} - |y|^\nu). \quad (\text{I2})$$

We can then work in polar coordinates and take $r = |y|$, which gives

$$\Omega_\perp(\mathcal{O}) = \int_0^R dr r^{N_{\text{IP}}-1} \delta(\mathcal{O} - r^\nu) \int_{S^{N_{\text{IP}}-1}} d\omega, \quad (\text{I3})$$

where we assume $R > \mathcal{O}^{1/\nu}$.

Standard identities allow the evaluation of Eq. (I3) as

$$\Omega_\perp(\mathcal{O}) = \frac{2\pi^{N_{\text{IP}}/2}}{\nu \Gamma\left(\frac{N_{\text{IP}}}{2}\right)} \mathcal{O}^{\frac{N_{\text{IP}}}{\nu}-1}. \quad (\text{I4})$$

-
- [1] G. James, ed., *Advanced Modern Engineering Mathematics*, fifth edition ed. (Pearson Education, Harlow, United Kingdom, 2018).
- [2] A. V. Oppenheim, A. S. Willsky, and I. T. Young, *Signals and Systems*, Prentice-Hall Signal Processing Series (Prentice-Hall, Englewood Cliffs, NJ, 1983).
- [3] K. Ogata, *Modern Control Engineering*, 5th ed., Prentice-Hall Electrical Engineering Series. Instrumentation and Controls Series (Prentice-Hall, Boston, 2010).
- [4] L. Debnath and D. Bhatta, *Integral Transforms and Their Applications*, 2nd ed. (Chapman & Hall/CRC, Boca Raton, Fla., 2007).
- [5] C. Moore and S. Mertens, *The Nature of Computation* (Oxford University Press, Oxford, 2011).
- [6] J. R. R. A. Martins and A. B. Lambe, Multidisciplinary Design Optimization: A Survey of Architectures, *AIAA Journal* **51**, 2049 (2013).
- [7] E. Polak, *Optimization*, edited by J. E. Marsden, L. Sirovich, and F. John, Applied Mathematical Sciences, Vol. 124 (Springer New York, New York, NY, 1997).
- [8] C. Shannon, A mathematical theory of communication, *Bell Syst. Tech. J.* **27**, 379 (1948).
- [9] J. Sethna, *Statistical Mechanics: Entropy, Order Parameters, and Complexity* (Oxford University Press, USA, 2021).
- [10] S. Kirkpatrick, C. D. Gelatt, and M. P. Vecchi, Optimization by simulated annealing, *Science* **220**, 671 (1983).
- [11] G. van Anders, D. Klotsa, A. S. Karas, P. M. Dodd, and S. C. Glotzer, Digital Alchemy for Materials Design: Colloids and Beyond, *ACS Nano* **9**, 9542 (2015).
- [12] M. Z. Miskin, G. Khaira, J. J. de Pablo, and H. M. Jaeger, Turning statistical physics models into materials design engines, *Proc. Natl. Acad. Sci. U.S.A.* **113**, 34 (2016).
- [13] P. Chitnelawong, A. A. Klishin, N. MacKay, D. J. Singer, and G. van Anders, No Free Lunch for Avoiding Clustering Vulnerabilities in Distributed Systems (2023), arxiv:2308.05196 [cond-mat, physics:physics].
- [14] H. Aliahmadi, M. Beckett, S. Connolly, D. Chen, and G. van Anders, Flashpoints Signal Hidden Inherent Instabilities in Land-Use Planning (2023), arxiv:2308.07714 [cond-mat, physics:physics].
- [15] S. Cabrera, I. Babayan, H. Aliahmadi, D. Chen, and G. van Anders, SLO/GO Degradation-

- Loss Sensitivity in Climate-Human System Coupling (2023), arxiv:2311.17905 [physics].
- [16] Y. Geng, G. van Anders, P. M. Dodd, J. Dshemuchadse, and S. C. Glotzer, Engineering Entropy for the Inverse Design of Colloidal Crystals from Hard Shapes, *Science Advances* **5**, eaaw0514 (2019).
- [17] H. Gould, J. Tobochnik, and W. Christian, *An Introduction to Computer Simulation Methods: Applications to Physical Systems*, revised third edition ed. (Amazon Fulfillment, Wrocław, 2023).
- [18] R. Cersonsky, G. van Anders, P. M. Dodd, and S. C. Glotzer, Relevance of packing to colloidal self-assembly, *Proc. Natl. Acad. Sci. USA* **115**, 1439 (2018), arxiv:1712.02473 [cond-mat.soft].
- [19] P. Zhou, J. Proctor, G. van Anders, and S. C. Glotzer, Alchemical molecular dynamics for inverse design, *Molecular Physics* **117**, 3968 (2019).
- [20] C. X. Du, G. van Anders, J. Dshemuchadse, and S. C. Glotzer, Inverse design of compression-induced Solid–Solid transitions in colloids, *Molecular Simulation* **46**, 1037 (2020).
- [21] E. G. Teich, G. van Anders, and S. C. Glotzer, Identity crisis in alchemical space drives the entropic colloidal glass transition, *Nat. Commun.* **10**, 64 (2019).
- [22] A. A. Klishin, C. P. Shields, D. J. Singer, and G. van Anders, Statistical physics of design, *New J. Phys.* **20**, 103038 (2018), arxiv:1709.03388 [physics.soc-ph].
- [23] A. A. Klishin, A. Kirkley, D. J. Singer, and G. van Anders, Robust design from systems physics, *Scientific Reports* **10**, 14334 (2020), arxiv:1805.02691 [physics.soc-ph].
- [24] A. A. Klishin, D. J. Singer, and G. van Anders, Avoidance, adjacency, and association in distributed system design, *J. Phys. Complexity* **2**, 025015 (2021), arxiv:2010.00141 [physics.soc-ph].
- [25] E. T. Jaynes, Information theory and statistical mechanics, *Phys. Rev.* **106**, 620 (1957).
- [26] D. Frenkel and B. Smit, *Understanding Molecular Simulation; from Algorithms to Applications* (Academic Press, 2002).
- [27] H. Aliahmadi, A. Sheedy, R. Perez, and G. Van Anders, Hyperoptimization insight for computational morphogenesis, (2024).
- [28] L. D. Landau and E. M. Lifshitz, *Statistical Physics, Part 1*, 3rd ed. (Butterworth-Heinemann, Oxford, 1980).
- [29] N. Goldenfeld, *Lectures on Phase Transitions and the Renormalization Group* (Addison-Wesley, Reading MA, 1992).
- [30] J. Zinn-Justin, *Quantum Field Theory and Critical Phenomena*, 4th ed. (Oxford University Press,

Oxford, 2002).